SANDIA REPORT

SAND2014-0192
Unlimited Release
Printed January, 2014

Characterization & Modeling of Materials in Glass-To-Metal Seals: Part I

Robert S. Chambers, John M. Emery, Rajan Tandon, Bonnie R. Antoun, Mark E. Stavig and Clay Newton

Prepared by
Sandia National Laboratories
Albuquerque, New Mexico 87185 and Livermore, California 94550

Sandia National Laboratories is a multi-program laboratory managed and operated by Sandia Corporation, a wholly owned subsidiary of Lockheed Martin Corporation, for the U.S. Department of Energy's National Nuclear Security Administration under contract DE-AC04-94AL85000.

Issued by Sandia National Laboratories, operated for the United States Department of Energy by Sandia Corporation.

Available to DOE and DOE contractors from
U.S. Department of Energy
Office of Scientific and Technical Information
P.O. Box 62
Oak Ridge, TN 37831

Telephone: (865) 576-8401
Facsimile: (865) 576-5728
E-Mail: reports@adonis.osti.gov
Online ordering: http://www.osti.gov/bridge

Available to the public from
U.S. Department of Commerce
National Technical Information Service
5285 Port Royal Rd.
Springfield, VA 22161

Telephone: (800) 553-6847
Facsimile: (703) 605-6900
E-Mail: orders@ntis.fedworld.gov
Online order: http://www.ntis.gov/help/ordermethods.asp?loc=7-4-0#online

SAND2014-0192
Unlimited Release
Printed January, 2014

Characterization & Modeling of Materials in Glass-To-Metal Seals

Robert S. Chambers
Component Science & Mechanics

John M. Emery
Solid Mechanics

Rajan Tandon
Materials Reliability

Bonnie R. Antoun
Mechanics of Materials

Mark E. Stavig
Organic Materials Science

Clay Newton
Materials Reliability

Sandia National Laboratories
P.O. Box 5800
Albuquerque, New Mexico 87185-MS0346

Abstract

To support higher fidelity modeling of residual stresses in glass-to-metal (GTM) seals and to demonstrate the accuracy of finite element analysis predictions, characterization and validation data have been collected for Sandia's commonly used compression seal materials. The temperature dependence of the storage moduli, the shear relaxation modulus master curve and structural relaxation of the Schott 8061 glass were measured and stress-strain curves were generated for SS304L VAR in small strain regimes typical of GTM seal applications spanning temperatures from 20 to 500 C. Material models were calibrated and finite element predictions are being compared to measured data to assess the accuracy of predictions.

ACKNOWLEDGMENTS

The authors would like to thank Mike Winter for the many helpful discussions and review of this this document. We also would like to thank the many Glass-To-Metal Seal customers who have motivated and supported the work.

Table of Contents

FIGURES

TABLES

1 INTRODUCTION

Glass-to-metal (GTM) seals are used to provide electrical connections to components that must be hermetically sealed. In a typical application, electrical connectivity is provided through metallic pins arranged within an opening of a metallic shell that is sealed with a glass to insulate/isolate the pin from the housing. During the sealing process, the glass is heated to its working point to allow it to flow, filling the voids between the pin and the housing. Then the entire assembly is cooled to room temperature. Because the glass, pins and housing materials have different coefficients of thermal expansion (CTE), residual stresses are generated during cool down and subsequent thermal cycling due to the mismatch in thermal strains accumulated at interfaces. If the mismatch causes excessive tensile stresses in the glass, imperfections can lead to cracks that compromise the hermeticity of the seal. A finite element model of a single-pin, concentric glass-to-metal seal is depicted in Figure 1.

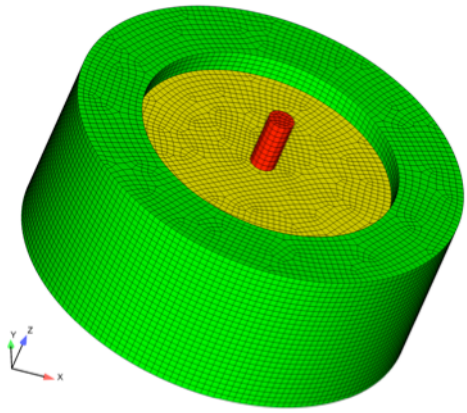

Figure 1 Finite element mesh of concentric, single-pin Glass-To-Metal seal

The choice of materials is an important factor in mitigating the risk of glass fracturing. By design, compression seals use an outer shell material with a CTE that is greater than the glass and a pin CTE that closely resembles or is less than the glass. As such, the glass is subjected to nominal radial compression on cooling that tends to reduce the likelihood of generating high tensile stresses. However, complex geometries still can experience cracking problems. One of the most common material combinations used by Sandia for a compression seal consists of a 304L stainless steel shell, Schott 8061 glass and alloy 52 pins.

Sandia has been designing, analyzing and building glass-to-metal seals successfully for many decades. However, as connector designs have evolved to more irregular shapes (e.g., lacking symmetry) and higher pin densities, the challenges of producing crack-free seals have increased. Furthermore, even the more straightforward designs experience unexplained glass fractures occasionally. Sometimes this is observed even when finite element stress analyses have predicted moderate to low tensile residual stresses. Although there are many possible explanations for these events, including anomalous processing and handling issues, questions have been raised about the fidelity of Sandia's residual stress predictions. Although advances in computational power have enabled the solution of larger boundary value problems with more

finite elements, advances in the fidelity of the requisite GTM seal material models have not kept pace. This is largely due to a lack of data and attention given to the materials, temperatures and strain regime experienced in compression glass-to-metal seals. Moreover, if the stresses are not computed accurately, then there is no hope of capturing the proper crack driving forces needed to support future fracture mechanics calculations. To remedy these deficiencies and methodically assess Sandia's ability to predict stresses in GTM seals, a combined experimental and modeling program is underway. This report provides an overview of that effort along with a summary of the data and results that have been generated thus far.

2 APPROACH

Historically, GTM seal analyses have been performed with finite element analysis codes using elastic material models for the glass and plasticity models for the pin and shells. This, of course, starts a long list of modeling assumptions that can affect the fidelity of the residual stress predictions. For example, glasses are not elastic materials. They are viscoelastic and undergo glass transition on cooling. If a glass is to be treated as an elastic material then a solidification, stress-free initial temperature also must be assumed. Geometric approximations (square corners) ignoring interfacial wetting and uniform processing temperatures commonly are assumed. Although judicious approximations may be entirely reasonable, there have been no attempts to prove them in a systematic study; nor have there been any serious attempts to adopt a more physically based material model for the glass. The essential features of the current research and development program are described below:

1) Fully characterize the behavior of the compression seal materials over the regimes critical to the generation of stresses from the glass sealing cycle. In general, this encompasses the temperature range from 500-600 C down to the lowest operating temperature (typically around -55 C). Since glasses are viscoelastic, it is important to characterize the time-temperature dependence driving stress relaxation as well as the thermal strain response under variable temperature histories (structural relaxation). Because yielding encountered in the pins and shell typically involves plastic strains of 1-2%, accurate data must be collected near the proportional limit at temperatures up to 500 C. To date, most of the SS304L data has been collected in support of ductile failure focusing on strains much higher. The small strain regimes have lacked sufficient fidelity for GTM seals.

2) Calibrate constitutive equations and validate material model predictions. Before trying to assess the fidelity of predictions in a structural analysis of a complicated GTM seal, it is important first to understand how well each material's stresses/strains can be predicted using the calibrated constitutive equations. This means characterizing materials, fitting material model parameters and using the constitutive equations to predict additional test data collected from material validation tests. The result is a quantitative assessment of the fidelity of the constitutive equations (e.g., small strain temperature-dependent plasticity, elasticity or viscoelasticity). Although Sandia implemented a viscoelastic material model for glass [1] many years ago, there has been no concerted effort to evaluate it due to a lack of data. In the intervening years, new viscoelastic constitutive equations have been developed for organic materials [2] that also may be applicable to the inorganic glasses. This project examines the applicability of both approaches.

3) Manufacture a representative GTM seal under well controlled processing and design/conduct tests to collect data on the residual stress/strain state for comparison to finite element analysis (FEA) predictions. After demonstrating the fidelity of the individual constitutive equations, the exercise now is repeated in a structural analysis of a well posed, initial boundary value problem for a GTM seal. This will assess the ability of the FEA to make consistent predictions in the presence of more complicated material interactions.

4) Assess sensitivity to modeling/processing assumptions. After demonstrating the ability to make accurate predictions in well controlled, well-defined GTM seal structures, it is important to assess the sensitivity of various modeling/processing assumptions. What are the realistic sealing geometries and sealing histories? How reasonable are modeling assumptions? How important is the glass meniscus from wetting? What happens if the cooling is not spatially uniform? This is an exercise to determine systematically what is important and what isn't when it comes to performing a FEA of a GTM seal.

A schematic overview of the modeling and testing roles within the R & D plan is depicted in Figure 2. This path will improve the fidelity of Sandia's GTM seal analyses, identify the most important aspects for modeling and quantify the effect of various modeling assumptions routinely made.

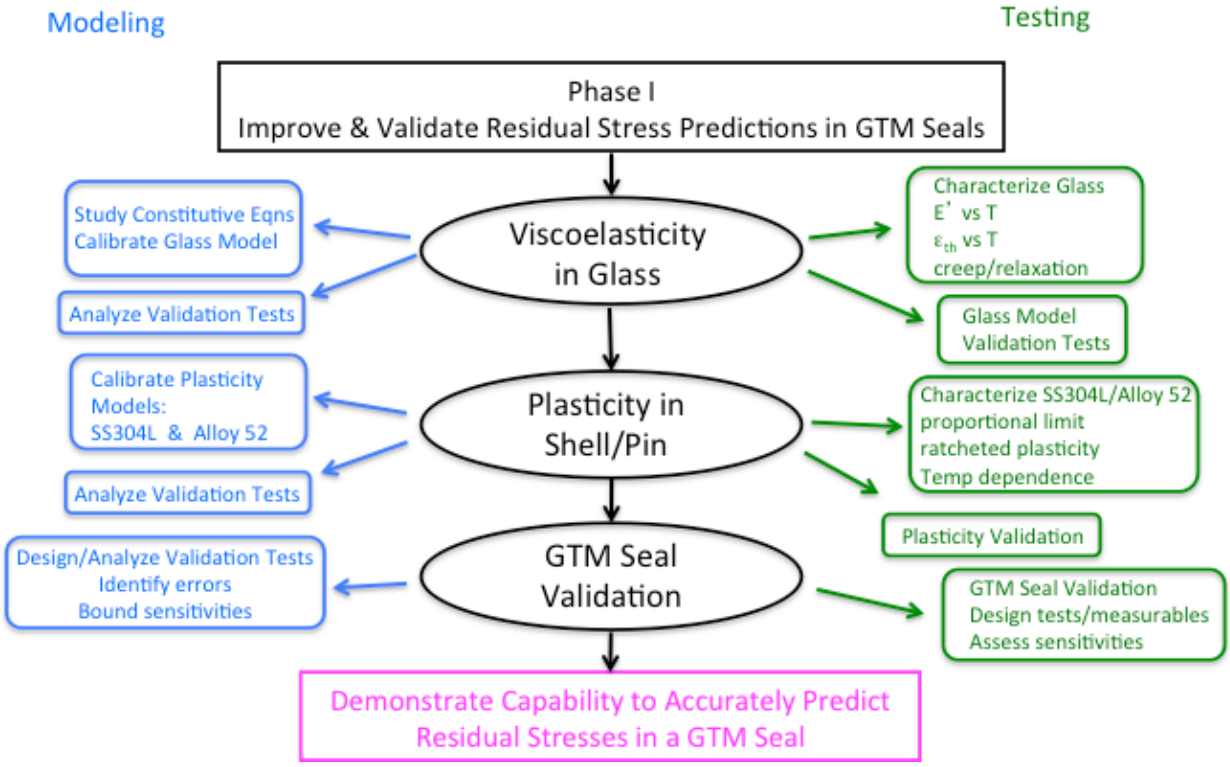

Figure 2 Overview of approach to demonstrate capability to predict residual stresses in GTM seals accurately

3 SCHOTT 8061 GLASS VISCOELASTICITY

Inorganic glasses are viscoelastic fluids. Although they appear solid-like at lower temperatures, they do experience a glass transition and on cooling attain a "rigid" condition (glassy state) without crystallizing. When reheated, the coefficient of thermal expansion (CTE) can increase by a factor of three as the material softens dramatically through glass transition, eventually even flowing under its own weight. Because glass stresses can relax quickly as the material flows above the glass transition temperature (Tg), GTM seals often are assumed to be stress-free in this regime.

Historically, analysts have simplified GTM seal analyses by assuming an abrupt glass transition at a discrete temperature set point (Tset) below which the glass is treated as an elastic solid. Under these conditions, the glass stresses can be computed based only on the elastic properties and thermal strain at the current state. There is no requirement to know anything about material history. However, it does require the analyst to define the initial stress-free temperature, Tset, and to be able to define the change in thermal strain from that state.

Although these assumptions make for quick and easy analyses, they do neglect certain aspects of the true material behavior. Because inorganic glasses are viscoelastic materials, they relax stresses over a broad range in temperature according to the imposed thermal history. Furthermore, thermal strain history generally cannot be calculated from a material property known as a thermal expansion coefficient. Just as the glass transition temperature (Tg) is a response affected by temperature history so is the thermal strain. In a properly constructed constitutive equation, the thermal strain history is calculated from the known temperature history, according to a mechanism known as structural relaxation.

To better understand the behavior of inorganic glasses in glass transition and to exploit opportunities to calibrate more sophisticated viscoelastic models for the glass, a set of experiments was designed and conducted. The goal was to characterize the time and temperature dependence of the S8061 glass including definitions of the two relaxation mechanisms, stress relaxation and structural relaxation.

3.1 Moduli Temperature Dependence

The initial glass tests were designed to define the temperature dependence of the "elastic" moduli. This was accomplished by measuring the in-phase and out-of-phase responses in a dynamic test imposing an oscillatory deformation at 1 Hz as the temperature was ramped from -80 C up to 500 C. Experiments were conducted in two different modes of deformation. The tensile moduli were measured in a 3-point bending test using the TA Q800 Dynamic Mechanical Analyzer. The shear moduli were measured under torsion in the TA ARES rheometer. Figure 3 and Figure 4 show plots of tan delta (loss/storage) and the in-phase storage moduli, respectively, as functions of temperature during the heating ramp. Most noticeable is the bump in tan delta at around 200 C. Historically, this feature would be considered too far below glass transition to be physical viscoelasticity, and yet it is consistently reproducible, occurring independently from any conditioning of the material (e.g., annealing, quenching). This may come from some

reproducible beta transition. Regardless, its occurrence seems to correspond to a change in temperature dependence of the storage moduli. Sealing glasses often are designated as "equivalent" materials based solely on comparable thermal strain behavior. In so doing, temperature dependent phenomena like this typically are overlooked.

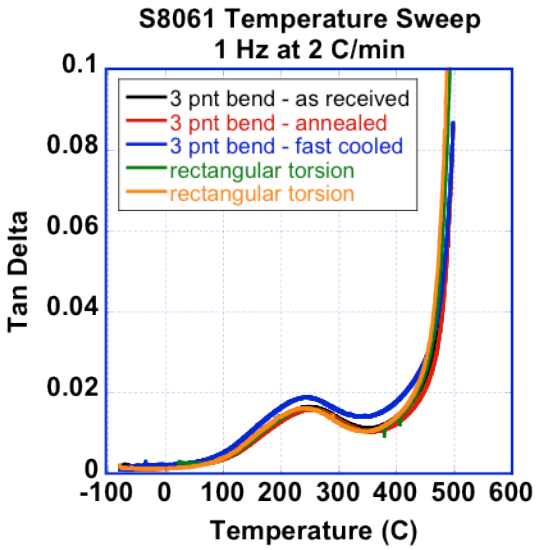

Figure 3 S8061 glass tan delta (loss/storage moduli) versus temperature

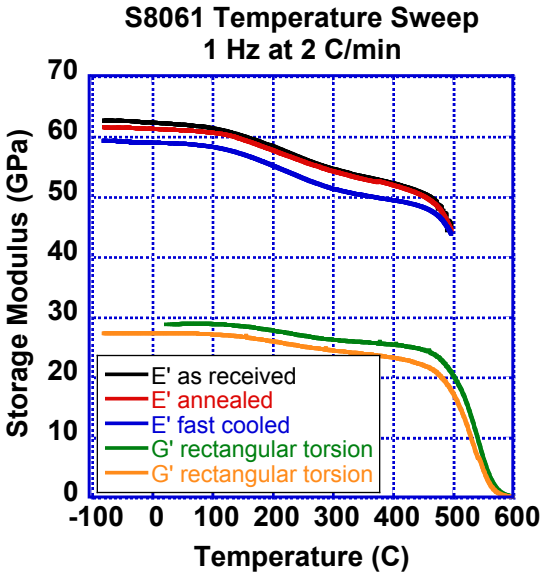

Figure 4 S8061 glass storage moduli versus temperature

The consistency of the temperature dependence can be seen by plotting the moduli normalized by the room temperature result. This produces a scale factor that varies from one at room

temperature down to 0.7 approaching 500 C (see Figure 5). By incorporating the change in moduli with temperature below glass transition, it should be possible to enhance the fidelity of elastic stress analyses.

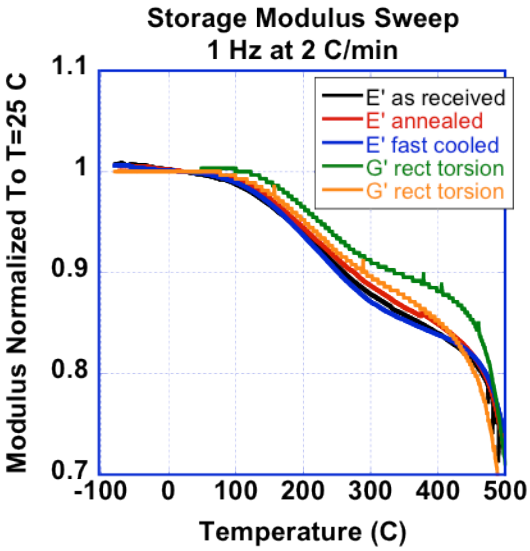

Figure 5 Storage moduli normalized by value at room temperature

3.2 Stress Relaxation Master Curves: Frequency Domain (Bending)

In a first attempt to collect data for a master curve in frequency space, the TA Q800 Dynamic Mechanical Analyzer was run with a single cantilever test sample to characterize the extensional modulus, E. Multiple tests were conducted each following a similar protocol: equilibrate at the initial temperature for 10 minutes; measure storage and loss moduli during a frequency sweep from 0.1 to 10 Hz; change temperature by a 10 C increment; equilibrate for 5 minutes; and repeat the frequency sweep and temperature increments until the programmed temperature range was covered. If the glass is thermorheologically simple, then the tan delta data for each frequency sweep at temperature can be shifted in log frequency space to obtain a master curve at some reference temperature, Tref. Since tan delta is computed from the ratio of loss modulus to the storage modulus, there is no vertical shifting required to accommodate modulus temperature dependence (i.e., it cancels out). When the storage modulus was plotted according to horizontal shifts in log frequency obtained from the construction of the tan delta master curve, there was a noticeable vertical offset. Normally, the vertical offset is attributed to a temperature dependence of the modulus. However, in this case, the shifts were much too large to be physically meaningful. Other explanations seemed much more likely including: slipping at the grips, deformation of the sample as it flows and changes shape or some other unexpected test artifact. Given the magnitude of these shifts, the data and master curves were considered to be unreliable.

3.3 Stress Relaxation Master Curves: Frequency Domain (Shear)

The 3-point bending, single cantilever beam and double cantilever beam test geometries all measure properties associated with the tensile relaxation modulus, E. Given the suspicious vertical shifts encountered in the master curve construction, it was deemed prudent to investigate other test geometries. That led to a study of torsion. Using the TA ARES rheometer, the same rectangular shaped glass samples (50mm x 11mm x 1.1 mm) were used, but this time they were subjected to torsional oscillations under the same protocol adopted for the single cantilever beam. Samples were equilibrated at temperature, subjected to a frequency sweep and then stepped in 10 C increments to the next temperature for a repeat. The tan delta data collected from this test geometry easily were shifted horizontally to obtain the master curve in Figure 6.

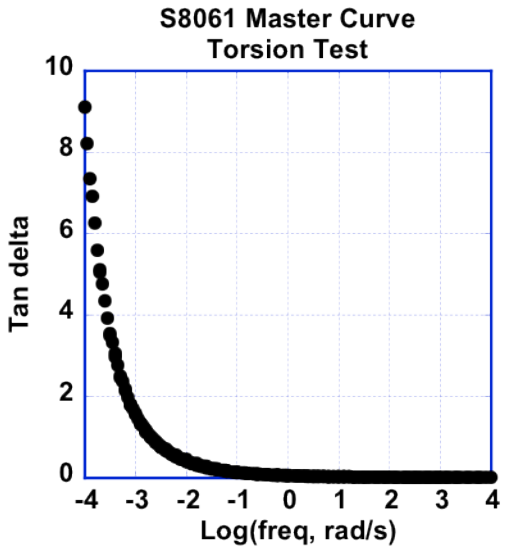

Figure 6 Shifted tan delta for S8061 torsion test with Tref=460 C

Empirical fits to the corresponding horizontal shifts are typically defined by a WLF [3] or an Arrhenius equation which relates the material clock to changes in temperature. These are provided in Eq. 1 and Eq. 2. Horizontal shifts from the fits and the data are plotted in Figure 7.

$$\log(a) = \frac{-17(T - 460)}{350 + (T - 460)} \quad T \text{ in Celsius} \qquad \text{Eq. 1}$$

$$\log(a) = (23452)\left(\frac{1}{T} - \frac{1}{733}\right) \quad T \text{ in Kelvin} \qquad \text{Eq. 2}$$

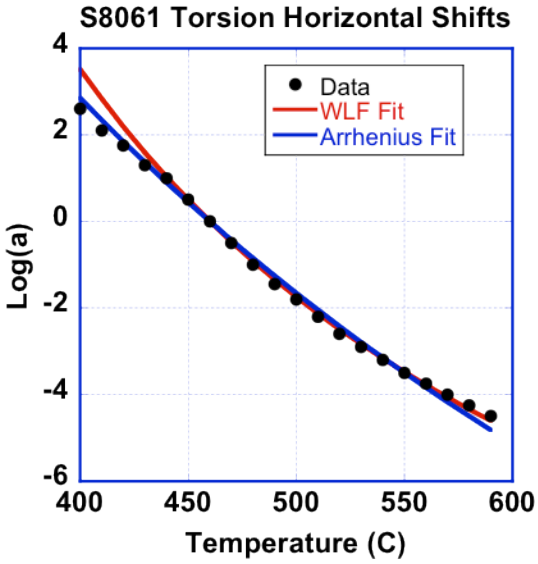

Figure 7 Horizontal shifts from tan delta in S8061 torsion tests with Tref= 460 C

When the horizontal shift factors were applied directly to the storage and loss shear moduli measured during the same test, the results in Figure 8 were obtained. Unlike the bending test results, no vertical shifts were required and the data aligned relatively smoothly. Some of the modulus scatter in the higher frequencies perhaps could and should be reduced by some small vertical shifts. Regardless, the important point is the enormous vertical shifts required for the extensional modulus from bending were not evident in the shear data. Although the reason for the large shifts necessary to fit the bending data is not known, the torsion experiments appear to have eliminated the issue in shear.

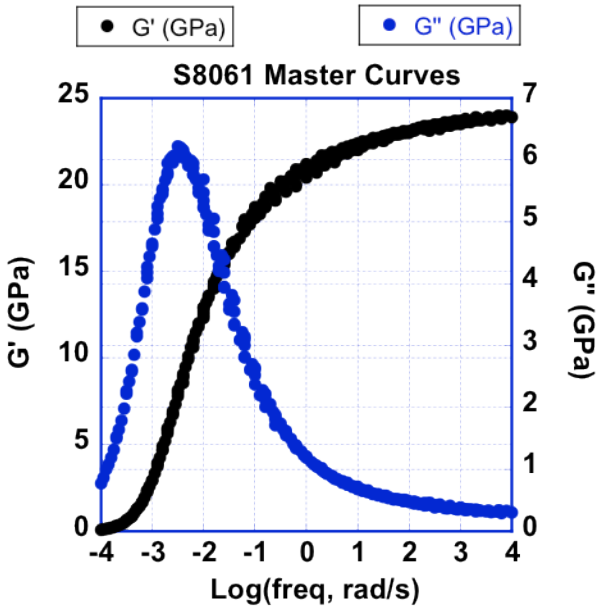

Figure 8 S8061 storage and loss shear master curves at Tref=460 C with horizontal shifts only

To confirm the reproducibility of the shear finding, the dynamic shear test was repeated. Once again selecting a reference temperature of 460 C, the new tan delta data were shifted in log frequency to obtain the master curve shown in Figure 9. The horizontal shift data and fits are plotted in Figure 10.

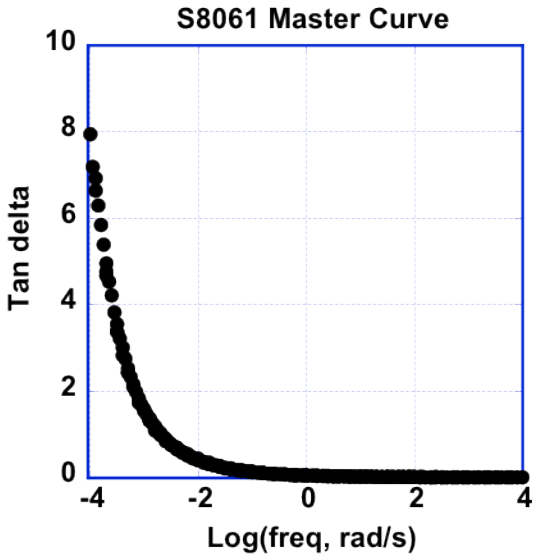

Figure 9 Shifted tan delta obtained from second torsion test with Tref= 460 C

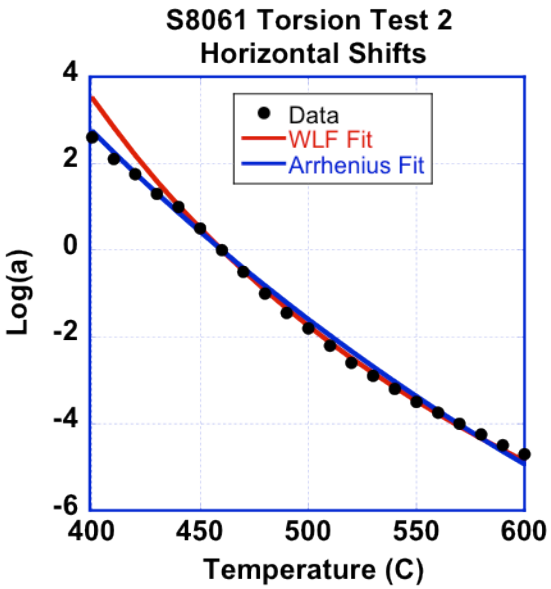

Figure 10 Horizontal shift factor obtained from second torsion test with Tref= 460 C

The WLF equation constants for this fit are the same as used in Eq. 1. The new Arrhenius pre-factor was reduced by about 4% as shown in Eq. 3.

$$\log(a) = (22584)\left(\frac{1}{T} - \frac{1}{733}\right) \quad T \text{ in Kelvin} \qquad \text{Eq. 3}$$

Following the same procedure used for the first torsion data set, the horizontal data shifts from Figure 10 were applied to the storage and loss shear moduli measured in the second test. These data are reported in Figure 11.

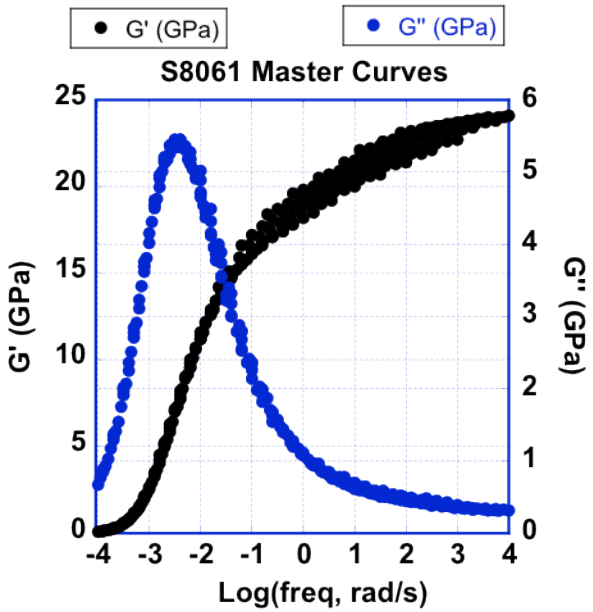

Figure 11 S8061 storage and loss shear master curves at T=460 C constructed from the second torsion test with only horizontal shifts applied

The second test results (with horizontal shifting only) show a noticeable scatter in the storage modulus at the higher frequencies. These data were significantly improved by allowing small vertical shifts. The improved master curves and the corresponding vertical shifts are plotted in Figure 12 and Figure 13, respectively.

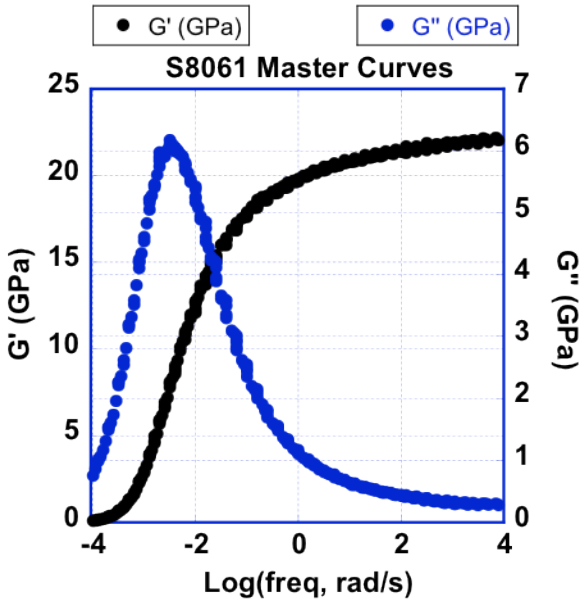

Figure 12 S8061 storage and loss shear moduli from second torsion test constructed at T= 460 C applying both horizontal and vertical shifts

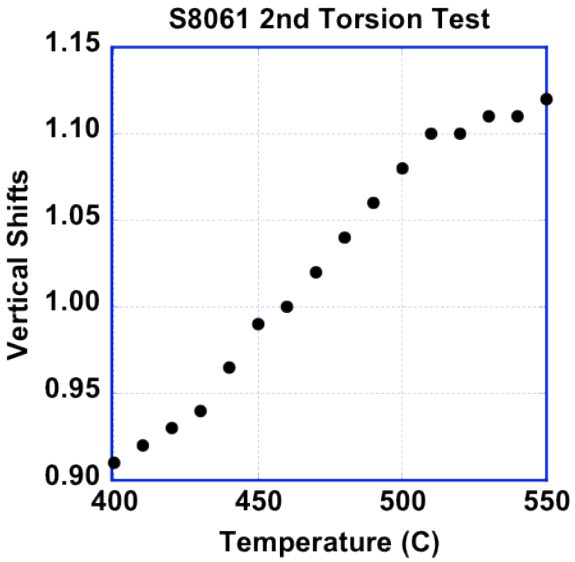

Figure 13 S8061 vertical shifts imposed on dynamic moduli from second torsion test

3.4 Mapping Shear Master Curves from Frequency to Time Domain

To use the master curve data in a finite element analysis, it is necessary to map from the frequency domain into the time domain. This is accomplished through a viscoelastic constitutive equation. For small deformations and constant temperature, the Boltzmann's superposition principle [4] can be used to compute the shear stress for an oscillatory shear strain:

$$\varepsilon_{xy}(t) = \varepsilon_o \sin(\omega t) \qquad \text{Eq. 4}$$

$$\sigma_{xy}(t) = \int_{-\infty}^{t} G(t-t') \frac{d\varepsilon_{xy}}{dt}(t')\, dt' \qquad \text{Eq. 5}$$

By substituting the derivative of Eq. 4 into Eq. 5 and making a change in variable whereby $s = t - t'$, the oscillatory shear stress can be written as

$$\begin{aligned}\sigma_{xy}(t) &= \varepsilon_o \left[\omega \int_0^{\infty} G(s) \sin(\omega s)\, ds\right] \sin(\omega t) + \varepsilon_o \left[\omega \int_0^{\infty} G(s) \cos(\omega s)\, ds\right] \cos(\omega t) \\ &= \varepsilon_o \left\{G' \sin(\omega t) + G'' \cos(\omega t)\right\}\end{aligned} \qquad \text{Eq. 6}$$

This equation defines the storage modulus, G', and the loss modulus, G'', in shear. For numerical integration purposes, it is attractive to define the relaxation functions as an exponential series expansion known as a Prony series:

$$G(t) = \sum_{i=1}^{N} g_i \exp(-t/\tau_i) \qquad \text{Eq. 7}$$

where g_i and τ_i are fitting parameters. Using Eq. 7 in Eq. 5 while applying the definitions of the storage and loss moduli in Eq. 6, the dynamic moduli can be written as an equivalent expansion in the frequency space:

$$G'(\omega) = \sum_{i=1}^{N} g_i \frac{(\omega\tau_i)^2}{1+(\omega\tau_i)^2} \qquad \text{Eq. 8}$$

$$G''(\omega) = \sum_{i=1}^{N} g_i \frac{(\omega\tau_i)}{1+(\omega\tau_i)^2} \qquad \text{Eq. 9}$$

By fitting Eq. 8 and Eq. 9 to the master curves in Figure 12, the Prony series coefficients, g_i and τ_i, can be defined. These are reported in Table 1. The comparisons of the resulting Prony series fits to the data for tan delta, the shear storage modulus, G', and the shear loss modulus, G'', are shown in Figure 14 and Figure 15. A substitution of those coefficients into Eq. 7 provides an expression for the shear relaxation function in the time domain. This shear stress relaxation modulus is plotted in Figure 16.

Table 1 Prony Series coefficients fit to tan delta from second torsion test

$g_i\,(MPa)$	$\tau_i(\text{sec})$
498	0.0001
365	0.001
519	0.01
778	0.10
1079	1
3283	10
4951	100
7805	316
3334	1580

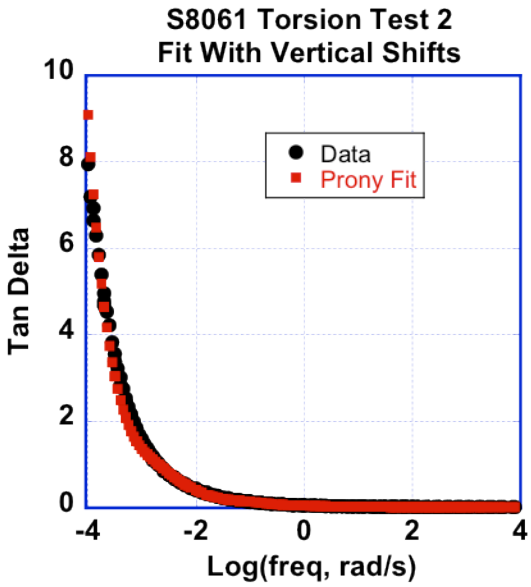

Figure 14 Prony series fit to the tan delta from the second torsion test with both horizontal and vertical shifts

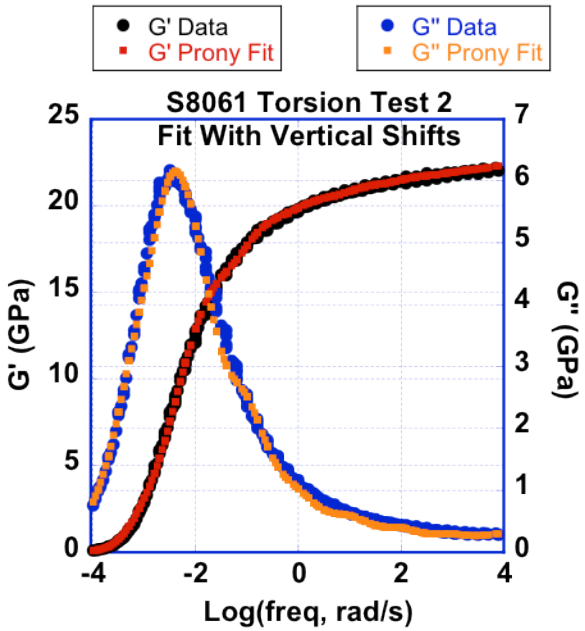

Figure 15 Prony series fit to the dynamic moduli from the second torsion test with horizontal and vertical shifts

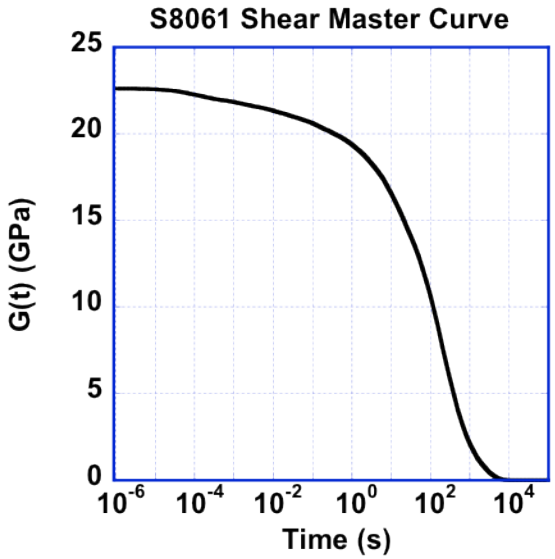

Figure 16 S8061 shear relaxation master curve at T=46 C constructed from the Prony series coefficients in Table 1

When the master curves for shear relaxation moduli from the two torsion tests are plotted together in Figure 17, the short time responses are seen to differ. Both the glassy modulus and the shape of the relaxation spectra can contribute to this effect. Here, the biggest contributor is the glassy modulus that varies by less than 10% (24.8 GPa in test #1 and 22.6 GPa in test #2). The normalized spectra, f(t)≡ $G(t)/G_g$, are plotted in Figure 18 and found to be similar.

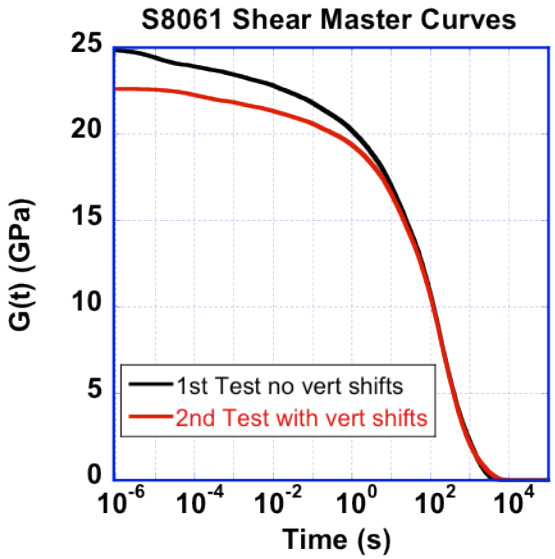

Figure 17 Comparison between the shear relaxation modulus master curves obtained from the two torsion tests: test #1 with horizontal shifts only and test #2 with horizontal and vertical shifts

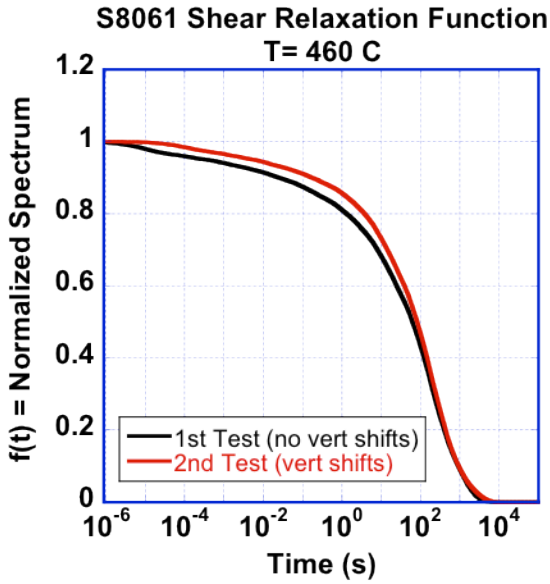

Figure 18 Normalized shear relaxation spectra from the two torsion tests

3.5 Direct Measurement of Torque Relaxation at Tref

The shear relaxation master curve was obtained by performing dynamic torsion tests and generating all results in the frequency domain. That required a mapping of the master curve from the frequency space into the time domain by the process described in the previous section. As a check on the validity and consistency of the above approach, torque relaxation tests were conducted at the reference temperature and surrounding temperatures to measure the time dependence of the shear relaxation modulus directly. If the material is thermorheologically simple then by shifting data to the 460 C reference temperature, the master curve should be reproduced. This is an independent check on the data. Torque relaxation tests were conducted at temperatures from 340 C to 460 C and the shifted data are plotted in Figure 19 along with the master curves obtained from the two torsion tests through dynamic testing. The agreement is excellent.

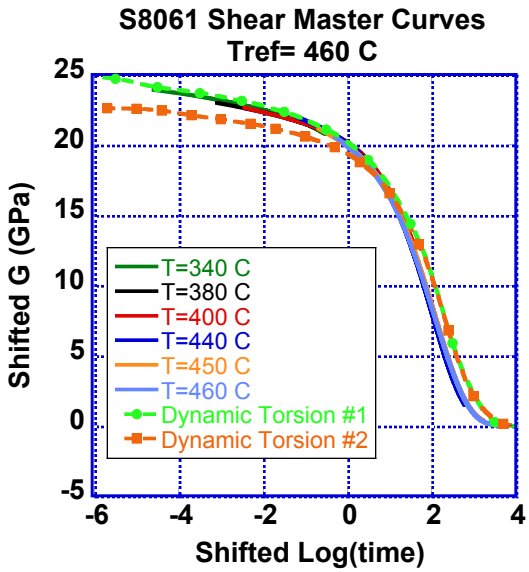

Figure 19 Comparison of shear relaxation master curves constructed from frequency domain and time domain

3.6 Bulk Response

Two material response functions are needed to define the stress-strain equations for an isotropic viscoelastic material. The torsion tests are sufficient to define the shear relaxation function, but one more definition is needed. Ideally, this would involve the pressure through the bulk relaxation modulus. However, these experiments are extremely difficult requiring a measurement of the long time equilibrium response in volume or pressure. As an alternative, assumptions were made about the functional form of the bulk response, and data were extracted from the literature to provide an initial estimate of the scaling between the glassy and equilibrium values of the bulk modulus. Thermal strain experiments then were used to modify the spectrum shape and adjust the bulk prefactors.

As a first approximation, the functional form of the normalized bulk relaxation function was assumed to have the same shape as the normalized shear response depicted in Figure 18. Even though the shape might be assumed to be the same, there is no requirement that the relative position in log time be identical. That is, spectra can be shifted relative to one another. This shift must be defined by other data, such as thermal strain versus temperature plots. The room temperature elastic moduli were computed directly from the measured glassy shear modulus (29.7 GPa plotted in Figure 4), using a Poisson's ratio of 0.22 taken from the Schott Glass 8061 technical data. This calculation yielded a tensile modulus of 70 GPa and a bulk modulus of 41.7 GPa, which compares favorably to the magnitude of the tensile modulus also reported by Schott (69 GPa).

Unlike the shear modulus, the bulk modulus does have an equilibrium value. Although the glassy modulus, K_g, can be approximated from published room temperature properties, the

equilibrium magnitude is a greater challenge. It is defined as the magnitude of the bulk modulus after all volume relaxations have occurred. From Corsaro data [5] for B_2O_3 bulk creep compliance, Rekhson [6] assumed a value of 3.3 for the ratio of glassy to rubbery bulk modulus. With this assumption, the room temperature equilibrium bulk modulus is estimated to be 12.6 GPa. The temperature dependence of the bulk modulus is more difficult to estimate. Although Figure 4 does give some data on the temperature dependence of the tensile and shear moduli, its affect on the bulk response is coupled. Clearly, the material becomes more incompressible above glass transition, but that is achievable naturally by a softening shear modulus with a large equilibrium bulk modulus. Since the thermal strain response as a function of different temperature histories is predicted by the bulk spectrum through the viscoelastic constitutive equations, the thermal strain experiments were used to deduce further information about all these parameters.

3.7 Structural Relaxation

Inorganic glasses cool to a rigid condition without crystallizing. As such, they are really frozen "liquids". At very high temperatures, glasses will flow freely to obtain the equilibrium state of a super-cooled liquid, but upon cooling, the increase in viscosity inhibits deformations. Eventually, rearrangements in the glass structure are unable to keep pace with the rate of cooling, and the material response departs from that of the super-cooled liquid. This marks the upper bound of the glass transition region. If cooling continues, there comes a state when the viscosity of the glass becomes so high that, practically speaking, the structural rearrangements cease. This defines the lower bound of glass transition where the true "glassy" state is attained. Glass transition is apparent when measuring the thermal strain during heating. Typically, the coefficient of thermal expansion changes by a factor of three as the material goes from the "glassy" state to the "liquid" as seen from the data slope in Figure 20. These measurements were made in a DIL 402 C Netzsch dilatometer. Because this is a contact measurement, a small load is used to keep the probe in contact with the sample. A typical sample has a square cross-section 5mm x 5mm and is about 25mm long. When loaded at about 15 centi-newtons, this results in an axial stress of around 0.006 MPa. At high temperatures, the sample tends to creep even under this small load accounting for the observed decease in CTE above 500 C.

Because of the role viscosity plays in inhibiting structural relaxation, thermal strain is a function of the temperature history and cannot be determined from the current state alone. This is clearly evident when cooling and heating a glass at different rates. In Figure 21, the thermal strains collected from two S8061 glass samples (5mm x 5mm cross-section, 25mm long) are plotted as a function of temperature. Each was annealed at 500 C, cooled at 0.5 C/min and then heated at 5 C/min. Even though the magnitude of the glass temperature change was the same for both heating and cooling, the shapes of the curves are different. Although the glass experiences the same temperatures on cooling and reheating, the effective dwell time is different at each temperature due to differences in heating/cooling rates. On cooling, there is more time for the structure to equilibrate at any given temperature. Hence, with the faster heating rate, it requires a higher temperature for the glassy structure to free itself (i.e., requires a lower viscosity at the shorter dwell time). Once the structure can relax, it asymptotes to the meta-stable equilibrium state of the super-cooled liquid and does so under a steeper return slope. That is what produces the "hysteresis" observed between the cooling and heating curves.

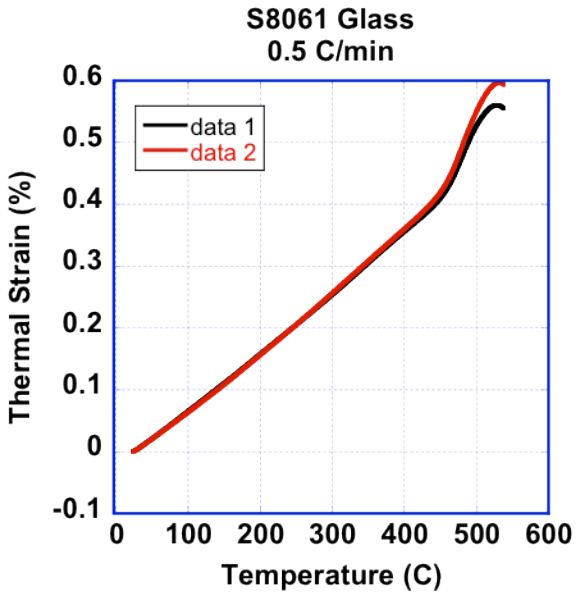

Figure 20 S8061 thermal strain data from heating at 5 C/min

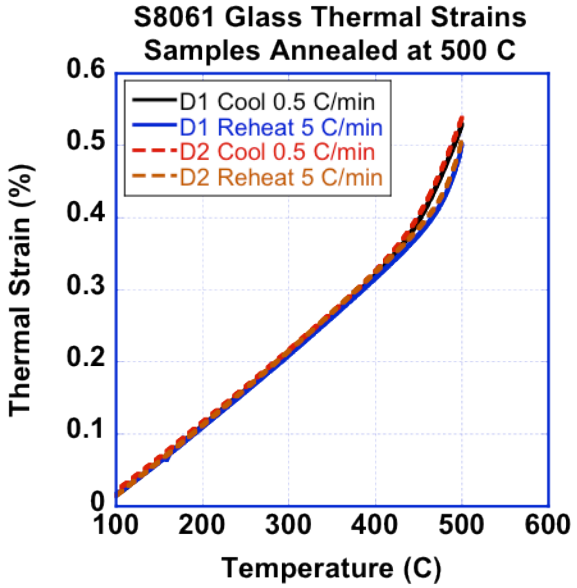

Figure 21 S8061 thermal strains after annealing at 500 C, then cooling at 0.5 C/min and reheating at 5 C/min

As another example of the unusual effects of structural relaxation experienced under different thermal histories, consider S8061 glass samples that have been annealed at 500 C for 30 minutes, rapidly quenched at 30 C/min to room temperature, reheated at 0.5 C/min to 500 C, annealed at 500 C for 30 minutes and quenched a second time at 30 C/min. Once again, two tests were

conducted with each sample 5mm x 5mm in cross-section and 25mm long. The measured thermal strains are plotted in Figure 22.

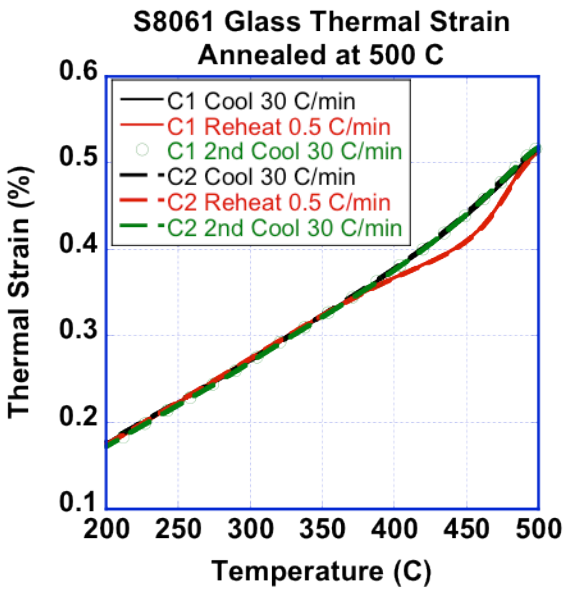

Figure 22 S8061 thermal strains after annealing at 500 C, then cooling at 30 C/min, heating at 0.5 C/min, annealing at 500 C for 30 minutes and cooling at 30 C/min

Because the 30 C/min cooling rate is so high, there is no apparent glass transition temperature (Tg) visible during cooling from 500 C (meaning the effective Tg would lie above 500 C). The glassy response at lower temperatures immediately is observed because starting from the equilibrated structure and viscosity at 500 C, the subsequent dwell times on cooling are insufficient for the structural re-arrangements to occur. During the reheating at a much slower 0.5 C/min, the glass has much more time at each temperature/viscosity for the structure of the glass to re-arrange as it strives to achieve the meta-stable equilibrium of the super-cooled liquid. This actually leads to an instantaneous coefficient of thermal expansion (local slope) in the range of 380-430 C that is less than the nominal "glassy" CTE. The heating rate curve does indicate a clear glass transition at around 460 C.

From these experiments, it is evident that the local strain behavior can vary under different temperature histories. The glass transition temperature is not a number but rather a structural response. Likewise, there is no constant material property that is a coefficient of thermal expansion (CTE). The thermal strain is a function of the structural state of the glass determined by prior temperature history. This can be an important consideration in residual stress analyses. If there are thermal gradients in the glass during the temperature regime surrounding glass transition, then the point-to-point thermal strains in the glass may be different. This is like having a material with a spatial variation in the coefficients of thermal expansion, and it produces additional stress from the local mismatch in strains under the changing temperature field. In fact, this is exactly the mechanism exploited in tempering glass plates where the surface is rapidly cooled and driven into compression by the delayed cooling of the interior. Elastic stress analyses are incapable of predicting this effect and necessarily assume the temperature field is spatially uniform and the CTE is prescribed.

One of the goals of this work is to collect data suitable for characterizing structural relaxation so it can be used to calibrate higher fidelity viscoelastic material models capable of predicting this behavior.

4 SS304L PLASTICITY

Most of the Sandia applications that have driven the characterization of 304L stainless steel involve very large deformations with special interest in exploring ductile failure. As a result, the experimental emphasis has focused on obtaining accurate stress-strain data to strains of order 1. In contrast, glass-to-metal (GTM) seals typically experience strains that are much smaller, on order of 1-2% from the glass sealing cycle. However, these plastic strains in the shell and pins can lead to substantial tensile stresses in the glass during subsequent unloading that occurs as the GTM seal is reheated during thermal cycling. Unfortunately, experiments designed to measure large strains at high temperature do not necessarily perform as well at small strains. For this reason, a considerable effort was devoted to developing a test apparatus to measure small plastic strains (<4%) from room temperature up to 500 C.

4.1 Small Strain, High Temperature Test Apparatus

Two approaches were investigated, but the one selected made use of a new, small strain extensometer (Model 3555-0050-004-HT) that can be placed directly into the furnace and used at temperatures up to 540 C. The extensometer has a gauge length of 0.5 inches and a travel of up to 0.02 inches (~ 4% strain). Although requiring a dedicated, factory calibrated signal conditioner, it uses a high temperature capacitive sensor and does not require any cooling. A photo of an instrumented sample is shown in Figure 23.

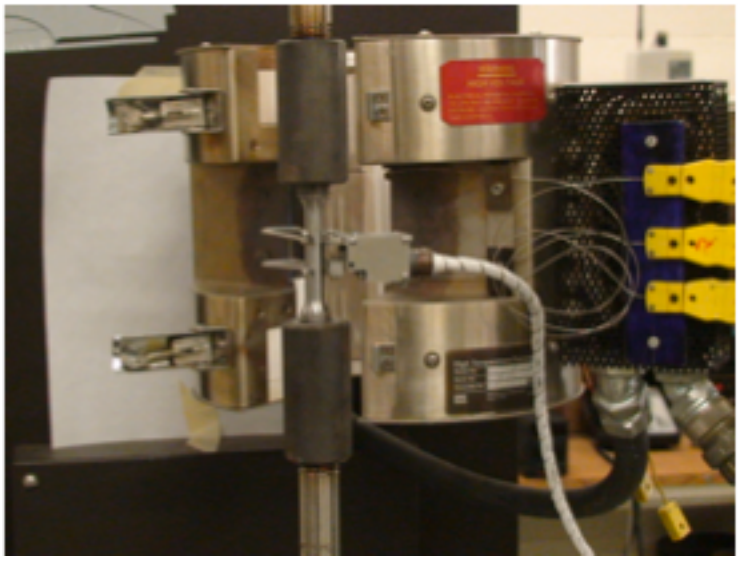

Figure 23 Extensometer mounted on sample for testing with environmental chamber shown in rear of photograph behind the furnace

4.2 SS304L VAR Stress-Strain Data

To maintain relevance with programmatic needs in GTM seal applications, two stainless steels were selected for testing, VAR (vacuum arc remelting) 304L and Carpenter P70, with the initial focus placed on the SS304L VAR material. Both 13" (MCN: 201252-201254, Heat No. 51511-1V, 51511-2V, 51511-3V weld critical manufactured by Electralloy and obtained from KCP, per specification 9800314) and 4" (MCN:201039:1 thru 12, Heat No. V3251-1, manufactured by Electralloy and obtained from KCP via Rocky Flats, per specification 9851812) bar stock were obtained and tested. The nominal diameter of the test specimens was 0.35" with a total gauge length of 1.5". The initial tests were conducted in strain control using the 0.5" extensometer at a strain rate of about 3E-5 s^{-1} similar to the strain rate expected in a GTM sealing operation. Figure 24 contains plots of the engineering stress-strain curves generated from the specimens machined from the 13" bar stock in the as-received condition. At temperatures of 300 C and above, there is clear evidence of strain aging or ratcheting that produces periodic load drops in the data. Although this can appear to be scatter or noise, it is a physical phenomenon that commonly occurs in 304L stainless steels at certain combinations of temperature and applied strain rate.

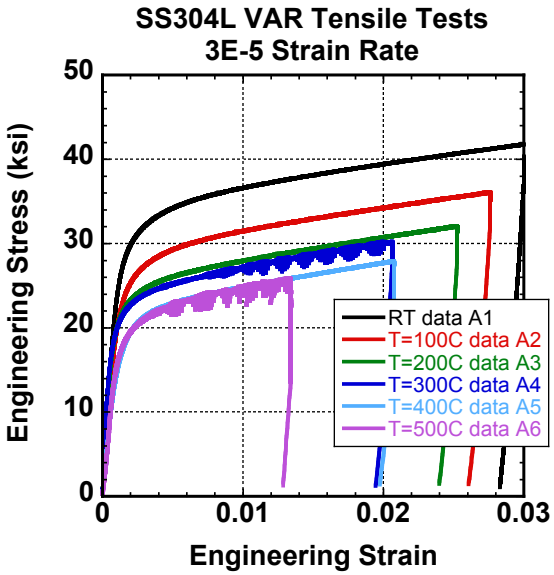

Figure 24 SS304L VAR stress-strain data from 13" bar stock as received (strain rate 3E-5 s^{-1})

To characterize the material more fully at these temperatures, post-yield stress relaxation data also were collected. In these tests, the strain was held constant while the force (stress) was measured as a function of time. The imposed strain history and corresponding stress relaxation are plotted in Figure 25 and Figure 26, respectively. It is quite apparent that even at room temperature, the yielded material exhibits significant stress relaxation over a period of minutes.

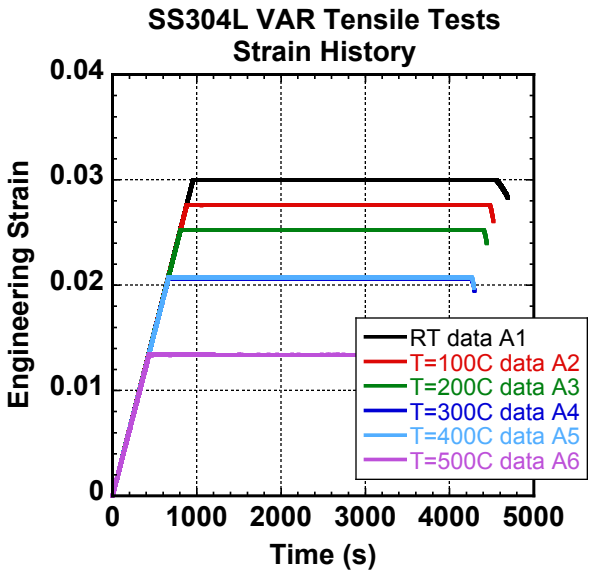

Figure 25 SS304L VAR strain history for stress relaxation on 13" bar stock as-received material

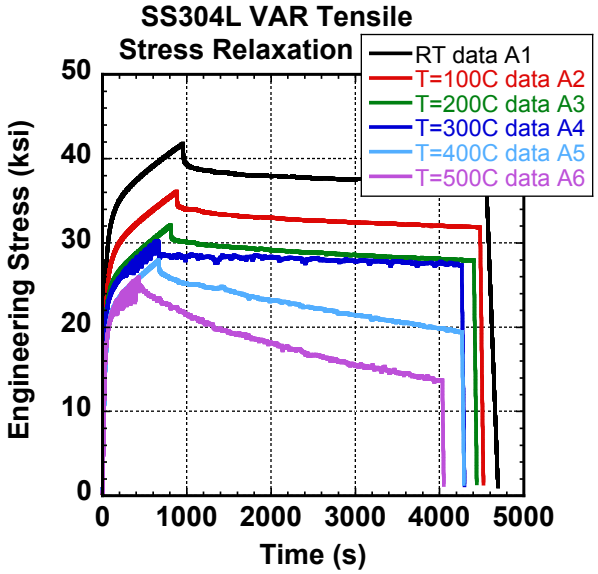

Figure 26 SS304L VAR stress relaxation in 13" bar stock as-received material

4.3 Annealing of the SS304L VAR During the Sealing Process

During the manufacturing process, the fixtured GTM assembly consisting of pins, glass preform and shell are subjected to temperatures high enough to allow the glass to flow sealing the gaps between pins and shell. It is the mismatch in thermal shrinkage during cool-down from these sealing temperatures that generates residual stresses in the GTM seal. Of particular interest is whether the exposure to these elevated temperatures is sufficient to further condition (i.e., anneal) the SS304L VAR shell material. To assess this, machined specimens were subjected to a typical glass sealing cycle before testing. Sealing cycles can vary, of course, from vendor to vendor and from glass to glass-ceramic. For this study, the slightly higher glass-ceramic sealing cycle was chosen. The test specimens were passed to an outside contractor for conditioning where they were to be heated to 990 at 25 C/min, held for 10-12 minutes at 990 C, cooled to 800 C at 10 C/min, ramped from 800 C to 482 C at 25 C/min, held at 482 C for 45 minutes and then ramped to 75 C at 15 C/min. When thermal traces were reviewed after product delivery, it was discovered that the specimens actually were held at 990 C for 35-40 minutes rather than the prescribed 10-12 minutes. Whether this makes a significant difference or not is unknown. Nevertheless, this is the conditioning of the materials whose results follow.

The stress-strain curves obtained from the specimens taken from the 4" bar stock after being conditioned according to the glass sealing cycle previously described are plotted in Figure 27. When these curves are compared to the curves in Figure 24 measured on the as-received condition of the 13" bar stock material, there are noticeable differences. Both the shape of the stress-strain response surrounding yielding and the magnitude of the yield strength are affected. After conditioning, the yield transition appears much more abrupt (i.e., more bilinear than rounded) and the yield strength appears lower. Moreover, the lowering of the yield strength seems to be more prevalent in the specimens tested at the higher temperatures.

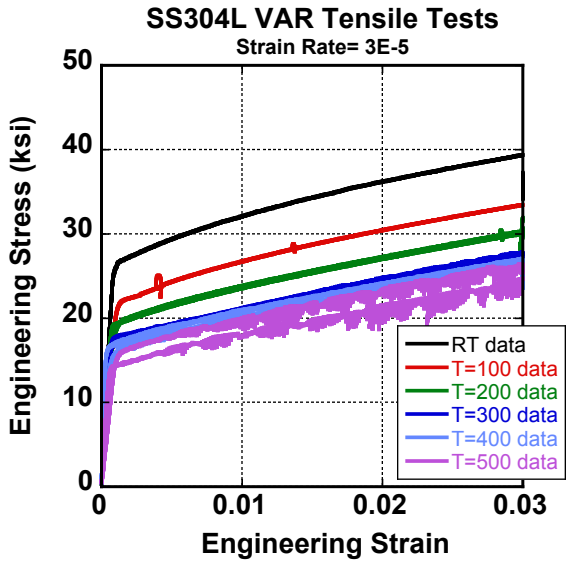

Figure 27 SS304L VAR stress-strain curves for material taken from 4" bar stock after exposed to glass sealing cycle (strain rate 3E-5 s^{-1})

The post-yield stress relaxation in the conditioned samples also was measured during the tests. This was done by stopping the applied deformation when the total strain reached about 3% and holding the strain level fixed allowing the force to relax. The stress response over time is plotted in Figure 28. Significant post-yield stress relaxation again is evident at room temperature after only a few minutes. Unlike the as-received material, these results show much less relaxation over comparable times at the higher temperatures.

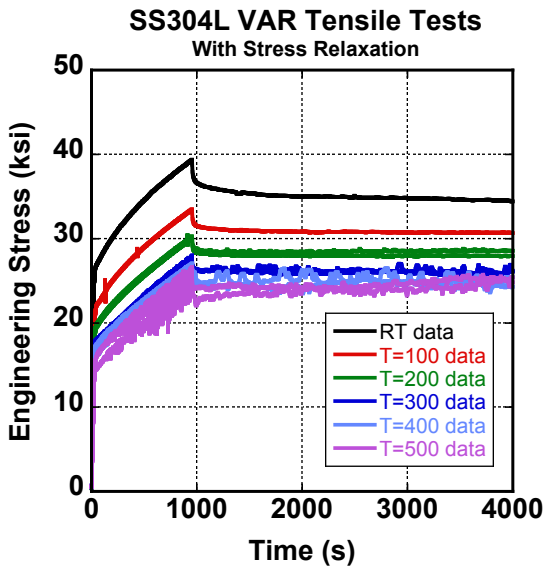

Figure 28 SS304L VAR stress relaxation at 3% strain in material taken from 4" bar stock after exposed to glass sealing cycle

5 S8061 NONLINEAR VISCOELASTIC MATERIAL MODELING

A physically based model of an amorphous glass must account for the viscoelastic behavior of the material. Although elastic material models have been used to predict residual stresses in GTM seals, they have done so by making subjective assumptions about the solidification and thermal shrinkage of the glass. Specifically, the analyst must choose a stress-free temperature called the set temperature, Tset, from which to begin the analysis. It is assumed that no stresses are generated above Tset because the glass is a fluid and able to freely flow relaxing all stress. Below Tset, the glass is assumed to behave as an elastic solid with a known correlation between the thermal strain and temperature. The effect of choosing a set temperature, typically around the annealing point of the glass, is to assume an instantaneous transition from the fluid to the solid glassy state at Tset. The relaxation data presented in the previous sections clearly indicate that the glass transitions more gradually. By adopting higher fidelity viscoelastic glass models the need for such assumptions is eliminated and opportunities are made available to investigate the details of glass processing.

5.1 Simplified Potential Energy Clock (SPEC) Model

In past years, a considerable effort was devoted to developing a nonlinear viscoelastic material model for the analyses of the glassy polymers used to encapsulate, bond and underfill components. Although most of these materials are glassy thermosets (crosslinked solids), they do exhibit many of the same behaviors seen in inorganic, amorphous glasses. Glass transition, stress relaxation and structural relaxation (physical aging) are common to both. Hence, even though another phenomenological viscoelastic model for inorganic glasses exists [1] and will ultimately be evaluated, there was considerable interest in determining whether one constitutive equation (SPEC model [2]) could be used to represent both the organic and inorganic glass forming materials.

The physical inputs to the material model revolve around four types of quantities: shear relaxation, bulk relaxation, thermal straining and the material clock. As with any viscoelastic formalism, the shear and bulk relaxation decay functions are defined at some reference temperature along with the glassy and equilibrium property coefficients and any temperature dependencies associated with these quantities. The shift factors for the material clock and the shear data have been collected and described in the previous sections, and an approach for acquiring the bulk representation also has been discussed. By comparing model predictions to the heating and cooling strains measured through glass transition, the remaining properties can be estimated and refined. That was the approach taken.

5.2 SPEC Material Model Predictions Compared to Data

Although a preliminary model calibration has produced a set of SPEC input parameters, these values are not unique as they were obtained by fitting the data available and not from a direct measurement of parameters obtained from a thorough suite of characterization tests. An evaluation of the quality of the material model predictions will determine the need for further refinement. That work is continuing. Note this is an important exercise that has been overlooked in the past as attempts have been made to evaluate GTM seal predictions without

first assessing the quality of the constitutive equations by comparing material stress-strain predictions to data. A summary of preliminary viscoelastic parameters is provided in the Appendix.

5.2.1 S8061 3-Point Bending Test

After characterizing some of the material properties of the glass, additional tests were undertaken to measure the structural response of glass samples loaded in 3-point bending under isothermal conditions at 460 C. In the first test, a glass beam 50mm long, 10.9mm wide and 1.09mm thick was loaded monotonically at 5 N/min to 18 N. Since the test temperature matched the reference temperature defined for the shear relaxation master curve, this data can be compared directly to a finite element analysis prediction using the measured master curve where real time and material time are equivalent (i.e., shift factor equal to one). The data fits for the second torsion test were used in analyses varying the number of elements through the beam thickness to assess the importance of mesh refinement. The finite element analyses were found to be quite insensitive to the mesh. Plots of the predictions are compared to the measured data in Figure 29. Excellent agreement was attained, providing further evidence for the validity of the material property characterization data. Although there was an apparent time dependence observed in the nonlinear force-deflection response because the viscoelastic glass was subjected to a relatively slow, 5 N/min, loading rate, the effect was fairly small. To determine the sensitivity of the model predictions to the value of glassy shear modulus, the analyses were repeated using the modulus measured in the first torsion test, 24.8 GPa. These results are compared in Figure 30. As expected, the shape is similar but the magnitude is changed.

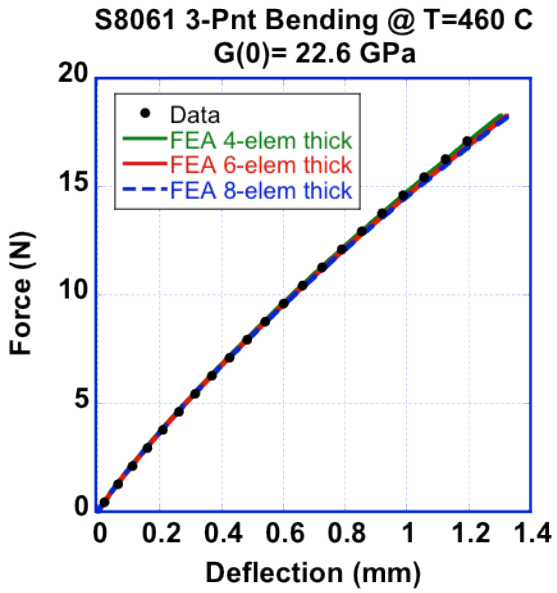

Figure 29 Comparison of finite element analysis predictions to 3-point bending test data at 460 C evaluating sensitivity of predictions to mesh refinement through the thickness of the beam

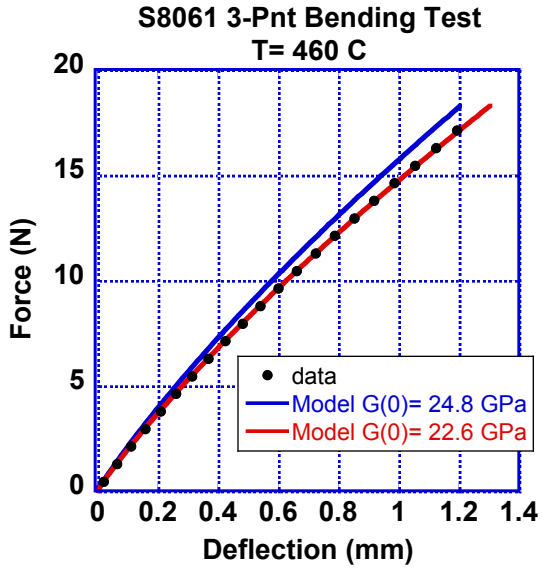

Figure 30 Comparison of finite element analysis predictions to 3-point bending test data at 460 C evaluating the sensitivity of predictions to glassy shear modulus

5.2.2 S8061 Complex Thermal Strain History with Structural Relaxation

As previously discussed, glasses undergo structural relaxation through the glass transition regime whereby the material seeks to attain the metastable equilibrium state of the super-cooled liquid. As a result, cooling at different rates can lead to differences in the apparent glass transition temperature as well as different changes in strain over the same temperature range (i.e., apparent differences in CTE). This also can cause the material volume to relax even at constant temperatures. To test the ability of the SPEC viscoelastic material model to predict such behavior, the thermal strains were measured under a complicated mixture of variable heating and cooling rates and temperature holds within the surrounding regime of glass transition. This time-temperature history then was prescribed in a one-element, finite element analysis to use the SPEC nonlinear viscoelastic constitutive equation to predict the corresponding strain history. The temperature history is plotted in Figure 31 and the comparison of SPEC model predictions to data is shown in Figure 32. The sample started from an annealed state in excess of 500 C and was cooled to as low as 330 C during the test. In all, the model predictions are quite reasonable and within the range of what would be considered engineering accuracy.

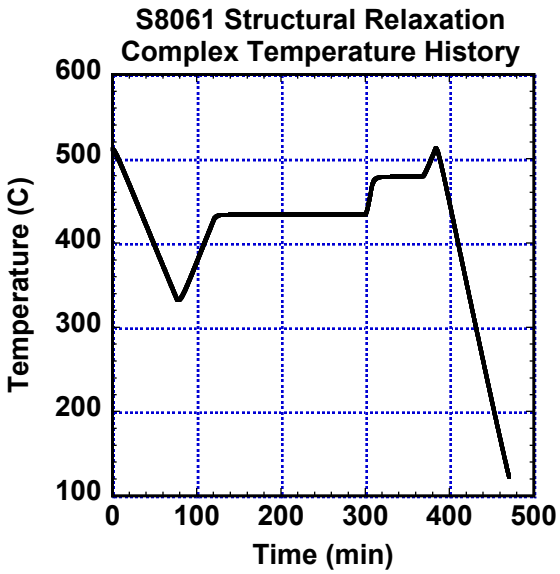

Figure 31 Definition of complex time-temperature history to evaluate thermal strain predictions

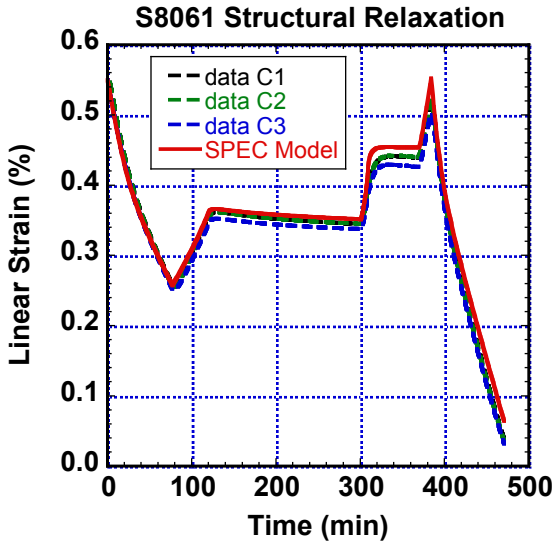

Figure 32 SPEC model predictions compared to S8061 thermal strain data from complex temperature history

6 SS304L VAR TEMPERATURE-DEPENDENT MATERIAL MODELING

The temperature dependence of the header material must be included in high fidelity predictions of residual stress for any GTM seal geometry. In the present document, the observed stress relaxation is not addressed; however, use of a time- and temperature-dependent viscoplastic constitutive model will be explored in the future. Here, the rate-independent, multi-linear elasto-plastic model is described and calibrated to the previously discussed experimental data. Then, simple but necessary verification tests are presented to demonstrate the ability of the model to reproduce the experimental data with finite element analyses.

6.1 Temperature-dependent, MultiLinear Elasto-Plastic (MLEP) Model

The temperature-dependent, multilinear elasto-plastic constitutive model is a J2 plasticity model that uses von Mises equivalent stress and requires input of the hardening response curves at various temperatures. The hardening response curves are input as x-y data pairs beginning at initial yield and zero plastic strain. For data at other temperatures, the model interpolates between the input response curves. The present data span room temperature to 100 C and up to 500 C at 100 C increments, *c.f.* Figure 27. To convert this data for use with the material model, the data are first smoothed to eliminate both fine scale noise and the oscillations associated with strain aging. For the higher temperatures where the effects of strain aging are particularly evident, the peaks of the oscillations are weighted more heavily in the smoothing process. After smoothing, polynomial splines are fit to the data and sampled to provide 1000, monotonically increasing data points. These data are then converted to true stress-strain assuming constant volume and translated to the hardening curve beginning at yield with zero plastic strain. The result for the data at a strain rate of 3e-5 s^{-1} is shown in Figure 33.

Following the material model calibration, a finite element model of the tensile specimen was generated and a calculation was made to repeat each tensile test, room temperature through 500 C. The FE model contained the nominal geometry of the tensile test and monotonic, longitudinal displacement was applied. A sample of the finite element model results for the 300 C calculation is shown in Figure 34. Only a 45° wedge of the circular cross-section was modeled and symmetry was used at the middle of the gauge section with appropriate boundary conditions. The figure uses reflection to portray the specimen with a longitudinal section and plots the von Mises equivalent stress contours. The outcome of the verification is shown in Figure 35 where the experimental data are plotted in red and fall nearly on top of the finite element calculations, plotted in blue. This is the expected outcome prior to formation of geometric instability.

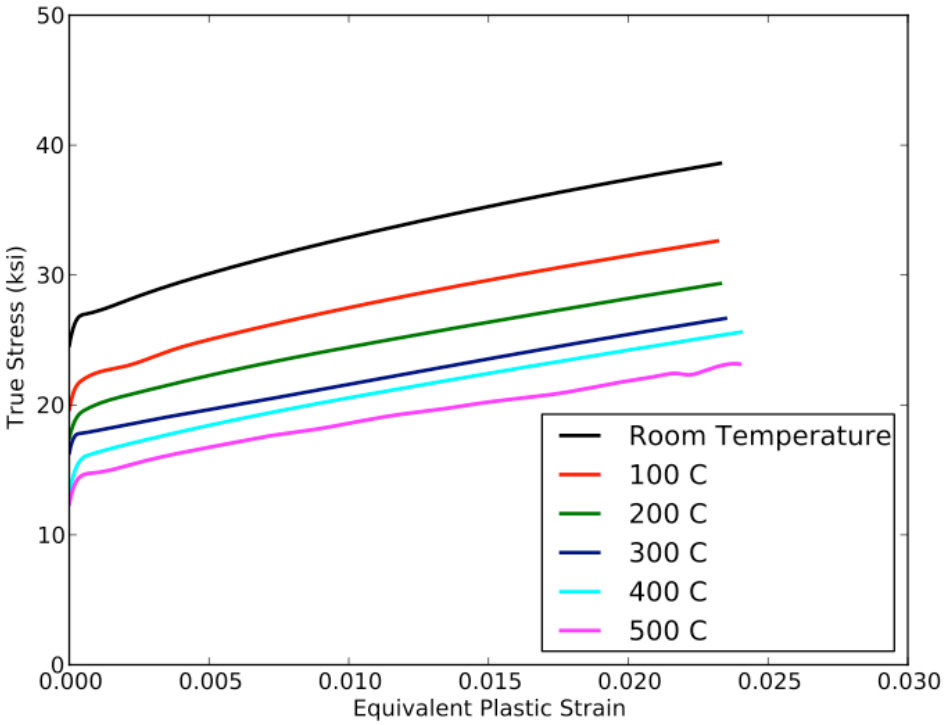

Figure 33 Hardening curves used as input for the temperature-dependent MLEP constitutive model

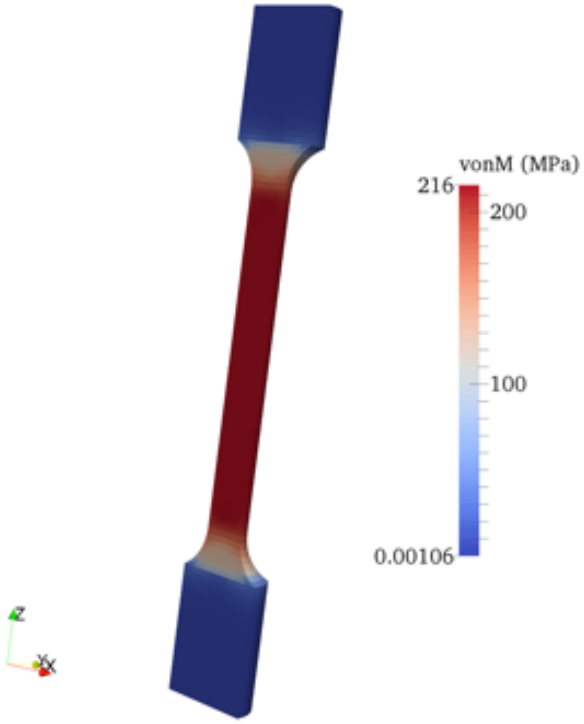

Figure 34 FE model replicating the 300 C tensile test showing uniform von Mises stress through the gauge cross-section under ~3.6% axial strain (units of stress are MPa)

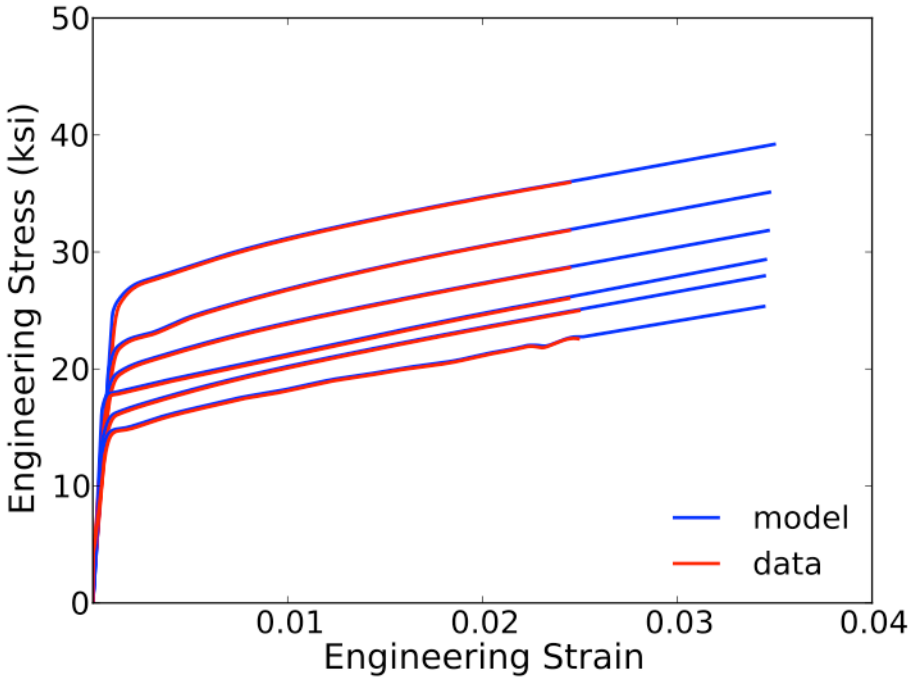

Figure 35 Engineering stress-strain plots comparing the experimental data (in red) to the finite element analysis predictions (in blue)

7 GTM SEAL VALIDATION TESTING

One of the greatest challenges facing this project is determining how to validate the residual stress predictions in glass-to-metal seals. To do so, some quantity must be measured and compared to a model prediction. Although finite element analyses predict the stress tensor at material points, experiments do not directly measure stresses. They may be inferred from collected data but that is based on assumptions that must be confirmed. Other quantities such as deformation and strain are predicted and indeed in some circumstances they are directly measureable. The problem, however, is the deformations and strains in a GTM seal are generated across a broad range of temperature starting as high as 500 C. To capture the whole process would mean an experimental apparatus would have to survive and perform precise measurements during this entire temperature span. That is beyond the reach of typical techniques (e.g., strain gauges). Moreover, to make valid comparisons between model predictions and measured data, the GTM seal must survive manufacturing without cracking, and the test conditions and geometry must be well known to define the initial boundary value problem. This effort just now is starting. In the following sections, some scoping experiments are described.

7.1 Indentation Tests to Infer Stresses from Crack Patterns

Indentation methods have been used to infer stresses near the surface of the glass by inducing surface cracks in a glass and comparing crack lengths to patterns generated in a stress-free sample (baseline). To begin scoping the sensitivity of this approach to distinguish stress differences generated by different processing conditions, a concentric GTM seal was studied. Existing samples were used to expedite the investigation. The nominal dimensions of the SS304L shell were 16 mm OD, 10.5 mm ID and 3.5 mm thick. However, since their processing history was unknown, it was necessary to reset the cooling history. That was accomplished by reheating the samples to 500 C and annealing for 30 minutes. Two cooling conditions were investigated, one slow cooled at 0.5 C/min to room temperature and the second pulled out of the oven for a rapid quench estimated at 100 C/min to 400 C. Because this is a compression seal that generated yielding in the shell, subsequent tensile stresses generated on reheating induced circumferential cracking close to the steel-glass interface. The cracking was identical for both the annealed and quenched samples. Since the purpose for this study was to assess the ability of indentation methods to detect differences in stress state (not to make quantitative predictions), the cracked seals were accepted for indentation.

These disks were indented with a Vicker's diamond indenter at 9.8 N load. Indentations were placed approximately equally spaced from about 500 microns from the interface to the center. The load chosen for this particular glass is such that the crack lengths on the base S8061 glass material are around 80 microns in size. Positive deviations from this crack size in the disk are indicative of local tensile stress, while negative deviations indicate compression. The images of these indentations on one of the disks are shown in Figure 36.

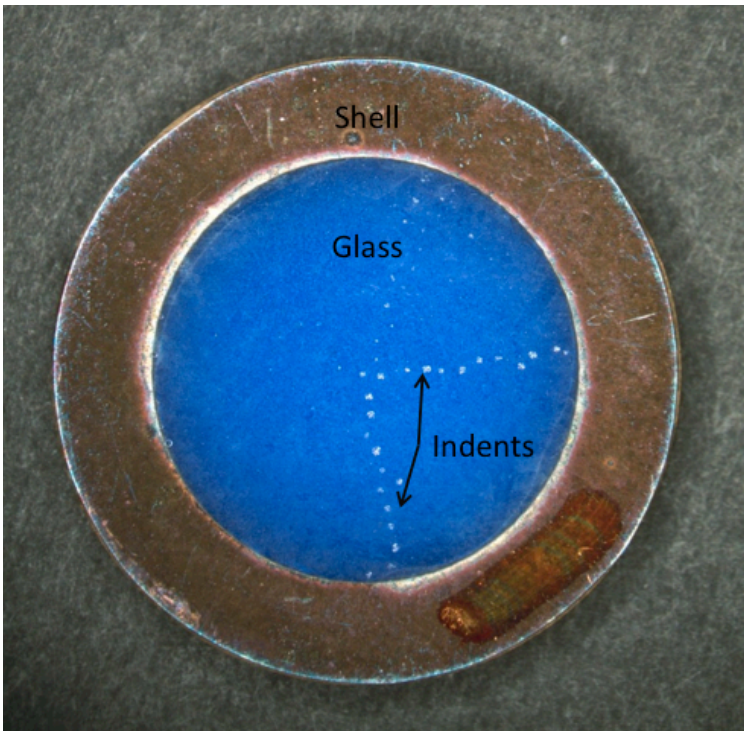

Figure 36 Concentric GTM seal with indentations on surface of the S8061 glass

Measurements of the crack lengths for each indentation were made, considering the following directionality: cracks parallel to shell are termed horizontal, while those perpendicular are called vertical. If the glass in the compression seal was uniformly compressed due to the thermal expansion mismatch with the shell so the radial and circumferential compressive stresses were equal, then the horizontal and vertical crack lengths would be expected to be identical and smaller than the stress-free, baseline glass cracks from indentation. Figure 37 shows higher magnification views of the crack, and the glass microstructure. Pores in the glass are observed, and the locations of the indentations are marked with the yellow arrows. An indent near the shell is shown in the red inset, while one near the center is shown in blue inset. Near the shell, the horizontal cracks on the indent are longer than the vertical ones, indicating either less compression, or perhaps even tension in the radial direction near the shell.

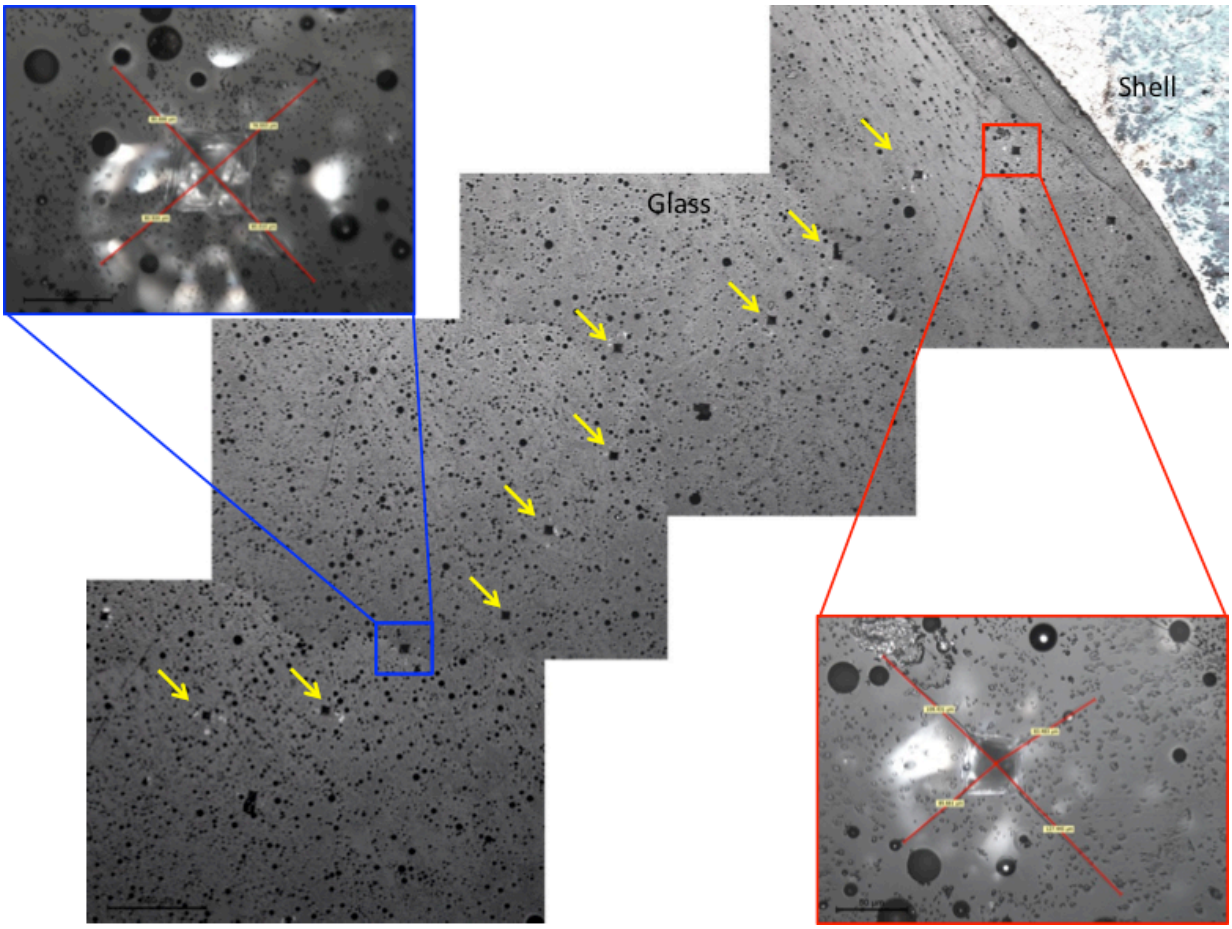

Figure 37 Higher resolution picture of the glass microstructure and cracking at indentations

Figure 38 plots of the vertical crack lengths (corresponding to hoop stresses) measured in both the annealed and quenched samples for comparison. Each data point is the average of two indents (four crack lengths). The values of the baseline are also shown. The crack lengths are slightly lower than the baseline close to the center, and there does not appear to be a large difference between the two disks tested. These crack length values are higher than measured in a similar disk which had not been annealed, indicating that some surface compression is relaxed by the annealing treatment. Based on comparison to the baseline, there appears to be only a slight compression in this seal in the circumferential direction.

Figure 39 shows measurements of the horizontal crack lengths (corresponding to radial stresses). While the annealed disk has almost negligible radial compression near the center, the quenched disk appears to have a slighlty higher compression, although due to scatter in the data, it is unclear if this can be stated with statistical certainity. Near the glass-steel interface, the crack lengths are significantly higher than the base for both disks, indicating that there is a radial tension in that region. This tension has not been affected by the heat-treatments, although the circumferential crack might have locally relieved the stresses.

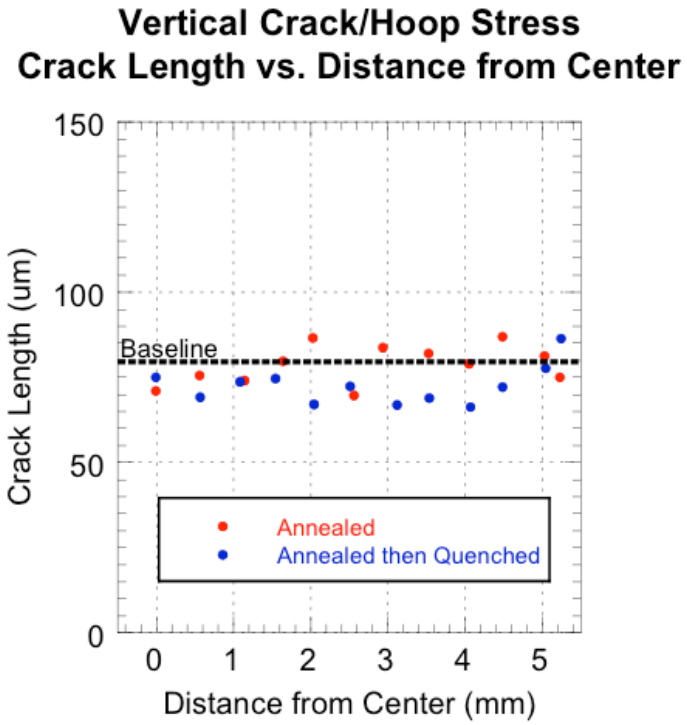

Figure 38 Comparison of vertical cracks generated in indentations on S8061 glass from annealed and quenched concentric GTM seals

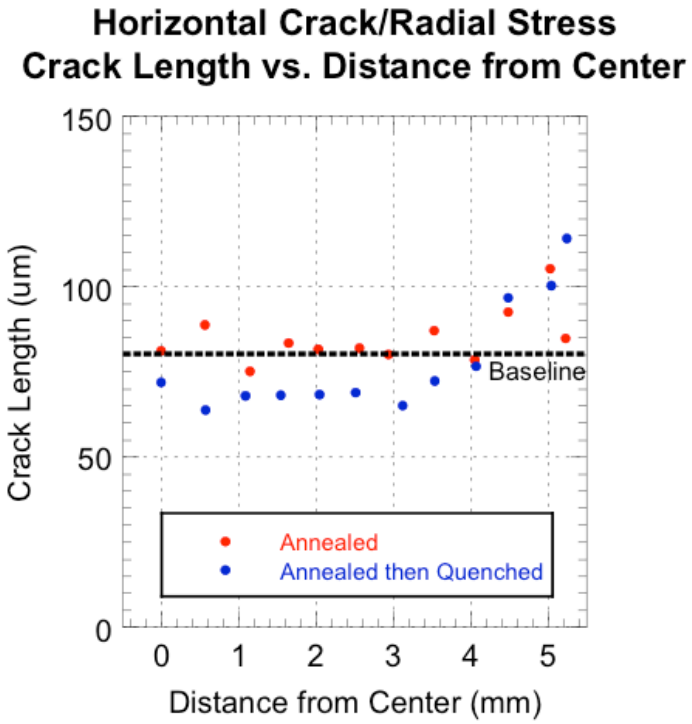

Figure 39 Comparison of horizontal cracks generated in indentations on S8061 glass from annealed and quenched concentric GTM seals

7.2 Other Test Methods for Generating Model Validation Data

While it is difficult to measure instantaneous changes in deformation during cooling from the high sealing temperatures, it is possible to measure curvatures and shapes at room temperature after sealing. That has lead to a consideration of bi-material beams or sandwich seals. If the glass does not crack and interfaces remain intact during cooling, then shape changes and curvatures created by the mismatch in thermal strains between the SS304L and the S8061 provide a possible metric for comparison to finite element predictions. Similarly, room temperatures samples can be instrumented to measure strains or deformations over smaller temperature changes around ambient conditions.

Other techniques might involve removing material on an instrumented sample. As an example, consider the concentric GTM seal in Figure 40. By instrumenting the shell with a strain gauge, the strains can be measured during moderate thermal cycling about room temperature. Depending on the thickness of the shell and the temperature cycle, this may lead to additional plastic straining. Alternatively, if the stainless steel is cut progressively through the shell thickness, the unloading path can be measured through strain gauges placed around the circumference of the shell. Other possibilities might include grinding away planes of material in an instrumented bi-material structure or even drilling out the glass in the concentric seal of Figure 40. Unfortunately, many of these approaches will need to be investigated just to determine what works well and what data is useful. Moreover, the experience of trial and error may be what is needed to spawn a novel idea.

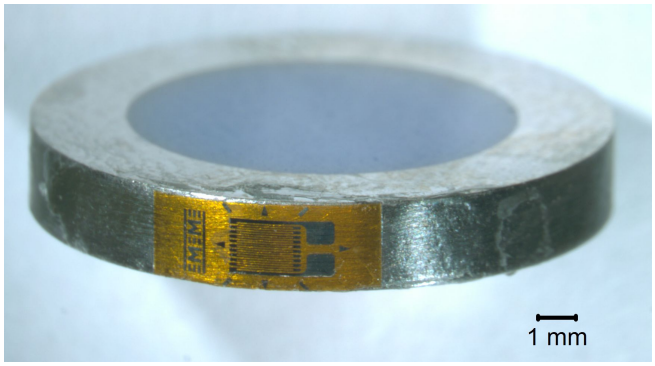

Figure 40 Strain gauges on shell of concentric GTM seal proposed for validation test (thermal cycling or cutting shell)

8 ACCOMPLISHMENTS

Although the work of characterizing glass-to-metal sealing materials, enhancing material models and validating constitutive equations and GTM seal analyses is not complete, many noteworthy accomplishments have been achieved:

1) A methodology and test specimen were designed to measure the frequency and time dependence of inorganic glasses and glass ceramics
    a. Have defined the shear stress relaxation master curve for S8061 glass
    b. This is a first for Sandia – have never had such data before
    c. Useful for defining glass solidification through higher fidelity viscoelastic models
2) The temperature dependence of the glass/glass-ceramic moduli have been measured in dynamic testing to obtain storage and loss moduli
    a. Have collected data from 3-point bending (E) and torsion (G) over temperatures ranging from -80 C to 600 C
    b. Assessed the sensitivity of moduli to glass processing and structure
3) Structural relaxation has been measured for S8061 glass defining thermal strain behavior under complex temperature histories
4) A new experimental apparatus has been developed to measure the small plastic strains (<4%), stress relaxation and stress-strain curves across temperatures from 20 C to 500 C
    a. SS304L VAR stress-strain curves have been measured from 20 C to 500 C
    b. Have quantified the effect of glass sealing cycle on the stress-strain curves of the as-received materials
    c. Post yield stress relaxation data has been collected from 20 C to 500 C
5) Material models for the SS304L VAR plasticity and S8061 glass viscoelasticity have been calibrated
6) Data have been collected to begin to validate the nonlinear viscoelastic glass model constitutive predictions
7) GTM seal tests are being investigated to identify a methodology suitable for validating GTM seal residual stress predictions

Perhaps, one of the most important consequences of this work is developing and demonstrating the methodology to affordably characterize the viscoelastic properties of Sandia's sealing glasses. With the right samples, the tests and data reduction can be performed on routine equipment in a matter of days. This is particularly important because it provides an efficient approach to evaluate a wider range of alternate sealing materials.

9 SUMMARY

Steps are being taken to improve and assess the fidelity of GTM seal stress analyses. For purposes of this study, two materials were selected from what are commonly used in a compression seal: SS304L VAR and Schott 8061 glass. Both materials and models are being evaluated by following a systematic approach consisting of the following steps:

1. Evaluate S8061 material behavior and model predictions (constitutive validation)
    a. Measure glass properties/behavior
        i. Temperature dependence of storage moduli (E' and G')
        ii. Viscoelastic shear relaxation behavior
        iii. Structural (volume) relaxation
    b. Calibrate glass constitutive equations
        i. Elasticity with temperature set point
        ii. Viscoelasticity
    c. Conduct validation tests on glass specimens with thermal and stress histories and compare measurements to finite element analysis predictions using calibrated glass models
2. Evaluate SS304L VAR material behavior and model predictions (constitutive validation)
    a. Measure metal properties/behavior
        i. Stress-strain curves from 20 C to 500 C
        ii. Post-yield Stress relaxation from 20 C to 500 C
        iii. Thermal strain response from -50 C to 700 C
    b. Calibrate thermal elastic-plastic constitutive equations
    c. Conduct validation tests on SS304L VAR specimens under various thermal and stress/strain histories and compare measurements to finite element analysis predictions using calibrated SS304L VAR model
3. Make and test glass-to-metal sealed structures (containing both materials) comparing measured responses to FEA predictions to assess accuracy of predictions and assumptions used in modeling (GTM seal validation)

Although work is continuing, substantial progress has been made in all three of the above areas as indicated by the accomplishments described in the previous section. Through the temperature dependence of the glass moduli (G and E), even an elastic GTM seal analysis can be improved by accounting for the gradual softening in the glass at temperatures approaching the temperature set point. Moreover, a more physically based understanding has been achieved in characterizing the time and temperature dependence of the shear stress relaxation modulus (G master curve) and structural relaxation through the thermal strain histories generated during solidification. With higher fidelity viscoelastic material models (SPEC and Narayanaswamy models), the actual thermal manufacturing histories including both spatial and temporal variations now can be simulated. When combined with plasticity models incorporating accurate stress-strain data collected in the small-strain regimes across temperatures spanning the glass sealing cycle, a higher fidelity GTM seal modeling capability is produced. This provides a platform for systematically evaluating traditional modeling assumptions and material parameter sensitivities.

To address the challenging task of assessing the accuracy of the finite element analysis predictions, the validation effort has been divided into two pieces. First, the constitutive equations themselves are being evaluated to determine how well they are able to predict the material behavior across the range of temperatures and deformations experienced by a GTM seal. Then, after demonstrating the accuracy of the material models, the quality of the finite element analyses of the more general boundary value problems associated with GTM seals can be addressed.

The task of validating viscoelastic glass model predictions was initiated by analyzing two tests: 3-point bending at 460 C and the thermal strains measured under complicated temperature histories varying heating and cooling rates. In both cases, the FEA results were found to compare favorably with measurements. Although the constitutive validation experiments for the SS304L VAR material have not been completed, the work of designing GTM test structures has begun. Indentation experiments were used to compare manufacturing stresses (inferred by crack patterns) generated in concentric GTM seals manufactured under different cooling cycles. In other experiments, similar seals have been strain-gauged to measure the change in strains induced by the removal of shell material during cutting. These efforts are ongoing.

10 REFERENCES

[1] Chambers, Robert S., "A Viscoelastic Material Model for Computing Stresses in Glass" (U), SAND90-0645, Sandia National Laboratories, Albuquerque, NM, July 1990
[2] Adolf DB, Chambers RS, Neidigk MA, Polymer 2009; 50:4257-69.
[3] Williams, ML, Landel RF, Ferry, JD, J. Amer. Chem. Soc, 1955; 77:3701
[4] Ferry JD, Viscoelastic Properties of Polymers, 1980, Wiley, NY.
[5] Corsaro RD, Phys. Chem. Glasses 1976, 17:13-22.
[6] Rekhson MS, Rekhson SM, J. Am. Ceram. Soc, 1986; 69:704-708.

11 APPENDIX: PRELIMINARY S8061 VISCOELASTIC PROPERTIES

.

Kg (GPa)	33
dKg/dT (MPa/C)	-20.5
Keq (GPa)	6
dKeq/dT	-5.9
$volumetric\ CTE, \propto_g\ (ppm/C)$	27
$volumetric\ CTE, \propto_{eq}\ (ppm/C)$	90
Gg (GPa)	24.95
Tref (C)	460
WLF C1	17
WLF C2 (C)	350
normalized bulk relaxation spectrum	$f(t) = e^{(-\frac{t}{30})^{0.3}}$
normalized shear relaxation spectrum	Table 1

DISTRIBUTION

1	MS0124	T. Aselage	8004
1	MS0145	D. Wall	1810
1	MS0343	A. Schauer	2610
1	MS0346	D. Peebles	1526
1	MS0346	R. Jamison	1526
1	MS0346	K. Ford	1526
1	MS0346	B. Elisberg	1526
1	MS0346	G. Winter	1526
1	MS0349	N. Lyon	2614
1	MS0349	E. Wilson	2616
1	MS0349	J. Bond	2614
1	MS0350	M. Stevens	2614
1	MS0350	M. Craig	2613
1	MS0350	G. Ely	2613
1	MS0350	D. Groysman	2613
1	MS0350	K. McCrory	2613
1	MS0350	M. Sena	2613
1	MS0350	S. Slszark	2613
1	MS0350	G. Benavides	2616
1	MS0350	J. Sment	2616
1	MS0352	E. Fang	1524
1	MS0386	T. Edwards	1527
1	MS0405	J. DeBassige	0433
1	MS0405	J. Kern	0433
1	MS0405	D. Lachowsky	0433
1	MS0405	J. McLaughlin	0433
1	MS0405	J. Olloway	0433
1	MS0405	S. Walker	0435
1	MS0405	T. Hinnerichs	0435
1	MS0481	R. Otten	2132
1	MS0523	J. Christensen	1733
1	MS0523	D. Luu	1733
1	MS0523	L. Andrews	1733
1	MS0525	S. Summers	1733
1	MS0555	T. Cordova	1521
1	MS0555	T. Cordova	1521
1	MS0557	C. D. Croessmann	1520
1	MS0557	D. Epp	1522
1	MS0557	T. Simmermacher	1523
1	MS0557	D. Epp	1522
1	MS0557	T. Simmermacher	1523
1	MS0614	D. Wesolowski	2545
1	MS0661	M. Neidigk	2627

1	MS0815	J. Johannes	1500
1	MS0836	C. Bourdon	1512
1	MS0840	D. Rader	1513
1	MS0840	J. Pott	1525
1	MS0840	L. Tuttle	1525
1	MS0886	L. Deibler	1819
1	MS0886	D. Susan	1831
1	MS0888	J. McElhanon	1835
1	MS0889	J. Glass	1818
1	MS0889	E. Reedy	1524
1	MS0889	M. Lane	1814
1	MS0889	R. Tandon	1818
1	MS0889	C. Newton	1818
1	MS0889	J. Puskar	1831
1	MS0889	J. Rodelas	1831
1	MS0889	B. Boyce	1831
1	MS0958	M. Kelly	1833
1	MS0958	M. Stavig	1835
1	MS0958	J. Kropka	1835
1	MS0959	S. Dai	1833
1	MS0982	J. Soelberg	1733
1	MS1064	L. Kashdan	2615
1	MS1135	R. Watkins	1532
1	MS1318	T. Trucano	1440
1	MS1349	W. Hammetter	1815
1	MS1349	K. Ewsuk	1815
1	MS1349	S. Reed	1815
1	MS1398	M. Neilsen	1526
1	MS1411	A. Sun	1814
1	MS1452	J. Norris	2552
1	MS1452	E. Dudley	2552
1	MS9042	M. Gonzales	8250
1	MS9042	C. Moen	8256
1	MS9042	B. Antoun	8256
1	MS0899	Technical Library	9536 (electronic copy)


Sandia National Laboratories